THESIS FOR THE DEGREE OF DOCTOR OF PHILOSOPHY

Recycling of TiO_2 Pigments from Waste Paint: Process Development, Surface Analysis, and Characterization

MIKAEL CARL FREDRIK KARLSSON

Department of Chemistry and Chemical Engineering
CHALMERS UNIVERSITY OF TECHNOLOGY
Göteborg, Sweden 2018

Recycling of TiO_2 Pigments from Waste Paint: Process Development, Surface Analysis, and Characterization
MIKAEL CARL FREDRIK KARLSSON
ISBN: 978-91-7597-722-5

Doktorsavhandlingar vid Chalmers tekniska högskola
Löpnummer: 4403
ISSN 0346-718X

Nuclear Chemistry and Industrial Materials Recycling
Department of Chemistry and Chemical Engineering
Chalmers University of Technology
SE-412 96, Göteborg
Sweden
Telephone: +46 (0) 31-772 1000

Cover: “Don’t cry over spilled paint” featuring Kathryn Janeway. Photo: T. Karlsson

Chalmers Reproservice
Göteborg, Sweden, 2018

Recycling of TiO_2 Pigments from Waste Paint: Process Development, Surface Analysis, and Characterization

MIKAEL CARL FREDRIK KARLSSON

Nuclear Chemistry and Industrial Materials Recycling
Department of Chemistry and Chemical Engineering
Chalmers University of Technology

Abstract

Pigments are commonly used in paint, plastic and paper products and titanium dioxide (TiO_2), the most important white pigment, accounts for approximately 70 % of the total volume of all pigments used today. Minerals containing TiO_2 are relatively abundant in the earth's crust. However, the production of TiO_2 is energy intensive and carries a high environmental burden. Therefore, the paint industry is seeking replacements for the virgin TiO_2 pigment used extensively in paint formulations today. The research work presented in this thesis was carried out to investigate the possibility to use secondary TiO_2 pigments, recycled from waste paint, as an alternative to virgin pigments.

Typically, commercial grade pigments are not pure TiO_2. Rather, they are surface treated in order to make the pigments more compatible with the paint matrix and to facilitate optimum dispersion. Waste paint feedstock for a recycling process will therefore contain TiO_2 pigments having different chemistries due to the variety of surface coatings. In this research three pigments, coated with different combinations of aluminium, silicon, and zirconium oxides were investigated.

The TiO_2 was recovered from paint in a three-step recycling process. First, the paint was pyrolysed at 500 °C in a nitrogen atmosphere to remove the volatile organic fraction. Next, the inorganic pyrolysed residues were oxidized in air at 500 °C to remove any residual organics and black carbon. After pyrolysis and oxidation the inorganic fraction was found to be contaminated with ionic salt residues from the decomposition of paint components during the recycling process. Therefore, the final step in the recycling process was to wash the residues in the presence of a mixture of ion exchangers yielding a pure secondary TiO_2 product.

In order to clarify the extent to which the pigment was affected by the recycling process, the characteristics of the recycled pigments were studied using techniques such as powder X-ray diffraction (XRD), X-ray photoelectron spectroscopy (XPS), and measurement of the dynamic electrophoretic mobility. Of the three pigments studied, it was shown that a pigment coated with a combination of silicon and aluminium oxides was more prone to degradation in the recycling process compared to pigments coated with a combination of aluminium and zirconium oxides or only aluminium oxide.

In addition, recycled pigment was used as a replacement for virgin pigment in a paint formulation. Results showed that the paint made from recycled TiO_2 had a minor decrease in opacity, and that the effect on whiteness was insignificant when compared to a paint containing virgin pigment. However, surface defects due to poorly dispersed pigments decreased the gloss of the paint film. Even though the performance of the recycled pigment was lower than that of the virgin pigment, it is suitable for use in applications such as low gloss formulations and ceiling paints.

Keywords: Paint, Pigment, Pyrolysis, Recovery, Recycling, Titanium dioxide, Waste.

List of publications

This thesis is based on the work contained in the following publications:

I. Karlsson, M. C. F., Corr, D., Forsgren, C., Steenari, B.-M. Recovery of titanium dioxide and other pigments from waste paint by pyrolysis. Journal of Coatings Technology and Research, 2015. 12(6): p. 1111-1122.

Contribution: Main author, all planning of experiments and analyses, experimental work and evaluation of data except paint formulation and evaluation which was done in collaboration with Akzo Decorative Paints.

II. Karlsson, M. C. F, Abbas, Z., Bordes, R., Cao, Y., Larsson, A, Rolland, A. Taylor, P. Steenari,B.-M.
Surface properties of recycled titanium oxide recovered from paint waste. Manuscript Submitted for Publication, 2018.

Contribution: Main author, all planning of experiments and analyses, all experimental work except model paint fabrication and XPS measurement. Evaluation of all data.

III. Karlsson, M. C. F, Abbas, Z., Bordes, R., Cao, Y., Larsson, A. Taylor, P. Steenari, B.-M.
Characterization of silicon, zirconium and aluminium coated titanium dioxide pigments recovered from paint waste. Manuscript Submitted for Publication, 2018.

Contribution: Main author. All planning of experiments and analyses, all experimental work except model paint fabrication and XPS measurement. Evaluation of all data.

IV. Karlsson, M. C. F, M., Álvarez-Asenciob, R., Bordes, R., Larsson, A., Taylor, P., Steenari,B.-M.
Characterization of paint formulated using secondary TiO_2 pigments recovered from waste paint. Manuscript Submitted for Publication, 2018.

Contribution: Main author. All planning of experiments and analyses, paint fabrication, measurement and evaluation of wet paint characteristics, gloss, colour and hiding power.

Preface

"…applied science is just as interesting as pure science, and what's more, it's a damn sight more difficult." -William. B. Hardy (1864-1934),

I don't think you will ever anticipate what you step into when you are starting your PhD program. All journeys from student to PhD are different and the ever-changing path is constantly hidden from the traveller in dark clouds of doubt and uncertainties. However, I can promise that the path will always be lined with new knowledge, valuable experiences and life-changing realizations.

This thesis summarizes my own journey. Expect no world changing document or a complete account of every aspect in the field of pigment recycling. Instead, my ambition with this thesis is the possibility of reaching out and bringing together representatives from the paint industry, the recycling companies and academia. I hope that this document sparks a flicker of interest in the reader. An interest that can lead to further development. Development that can lead to the better utilization of pigments, waste handling of paint or wherever the imagination of the reader dares to venture.

/Mikael Karlsson, 2018-04-06 Göteborg, Sweden

Funding

This work was funded by the Swedish Governmental Agency for Innovation Systems (grant number: P37547-1), Akzo Nobel Decorative Paints, UK and Stena Metall AB Sweden.

Scholarship was granted from the Swedish Paint and Printing Ink Makers Association and the Swedish Adhesive and Sealants Association, Chalmers Competence Centre of Recycling and the graduate school Polytechnic Waste Research in Sweden

Acknowledgements

There are numerous people that made this thesis possible and deserves my thanks. I especially want to thank (in no particular order):

Toni the most beautiful, caring, intelligent, and funniest person I ever meet, the complete package! My wife and my best friend. Know that this thesis wouldn't be possible without you.

My supervisor Britt-Marie Steenari for believing in me, teaching me all I know about recycling and letting me choose my own path. "This book was written using 100% recycled words." - Terry Pratchett

My examiner Christian Ekberg for your feedback and input. Your facial hair is an inspiration to us all.

My co-supervisor Stellan Holgersson always there with a helping hand when needed and for being the "common sense" of the department.

Phil Taylor for all your support, positivity, and enthusiasm.

Ana-Martha Coutino for a life cycle perspective.

Christer Forsgren as you were the one who originally came up with the idea that led to this project.

Zareen Abbas for your unconditional help, for pointing out my mistakes, and your sense of detail.

Romain Bordes for your passion and our brainstorming moments.

Anders Larsson for your encouraging words and your knowledge in paint chemistry.

Yu Cao for always being so helpful, and always with a smile on her face.

Kim Henriksson for support with pilot pyrolysis experiments.

Michael Persson for his genuine interest in this project.

Neil Rowson, Mirja Illikainen, João Labrincha, Cecilia Groth and Monica Billger for evaluating this work.

My friends and colleagues at industrial materials recycling and nuclear chemistry. You are a diverse group with different backgrounds and motives which creates a most stimulating workplace. You are all special to me.

All the personnel at Akzo Nobel Decorative Paints who welcomed me with open arms. Especially Daniel Corr, John Steele, and Emma London.

The personnel at Akzo Nobel Performance Additives for letting me borrow your lab. A special thanks to Maria Stjerndahl and Margareta Maggan Persson.

My former colleagues at Flügger who sparked my interest and showed me the importance of paint chemistry. I miss you all.

My students Carolina Enge de Carvalho, Antonin Rolland and Frida Petrusson. Sometimes it just feels good to have someone to boss around.

Kathryn Janeway (the cat, not the Vice Admiral) for being your annoying, hairy but lovely self during this whole stressful process.

You, as a reader, for being curious about this work. Together we can strive to make the world a more safe, sustainable, and happy place for everyone.

Table of Contents

1. Introduction

In today's society, paint and coatings have many technical applications and are found the world over. They are used to increase the life-time of products and infrastructure, such as buildings and bridges, reduce the growth of barnacles on the bottoms of ships or to tailor-make the adhesion between surfaces. In addition, coatings are also aesthetically important due to their ability to provide colour. Different colours create different feelings or associations, and at the same time colours can also make written messages more accessible and make a room feel more or less illuminated.

Coatings with different colours are produced by using various pigments. Pigments are diverse and can be of both an organic and inorganic origin, however, the by far most commonly used pigment is the white pigment titanium dioxide (TiO_2). TiO_2 became commercially available in 1916 but it was not until the toxicity of the lead based pigments was understood in the 1950's that TiO_2 became popular. By the 1970's TiO_2, was the most important pigment used by the coatings industry due to its abundance and its ability to scatter visible light while being chemically inert [1]. Today, TiO_2 accounts for approximately 70% of the total volume of all pigments used [2].

TiO_2 is often mentioned as the major white pigment, but commercial grade pigment is frequently not pure TiO_2. The crystalline TiO_2 core is the active ingredient that provides the pigment's optical functions. However, the surface of the TiO_2 particles does not consist solely of titanium and oxygen. As the TiO_2 crystals grow during manufacturing, insoluble components accumulate on the surface. These components can be contaminants from the ore or additives added deliberately to control the crystal structure or crystal growth during manufacturing [3, 4]. Besides these impurities, the surface of a pigment is often deliberately altered to suit the final application of the pigment. To reduce photoactivity and to improve the compatibility between the pigment and the other paint components, the surface of the TiO_2 pigment is usually treated with silicon, aluminium and zirconium oxides. Uncoated TiO_2 pigment shows a complex behaviour with different active groups on the surface, but a coated pigment can have an even more complex surface that is chemically very different to the bulk TiO_2 phase [5]. For the optimum opacity and durability of a paint film, a well dispersed pigment is a must. So, although it is not an uncomplicated task, the surface characterization of a coated pigment is of importance in understanding pigment-medium interactions and the performance of the pigment in a paint system [6].

Typically, TiO_2 is produced from ilmenite minerals using a sulphate or chloride route, both of which have a high carbon footprint per kilogram of TiO_2 produced. It has been reported that even if new innovative production routes are developed, the carbon footprint per kg TiO_2 produced would still be high [7]. The European Union (EU) has recognized the environmental impact of TiO_2 production and has consequently set restrictions on the amount of TiO_2 allowed to be used in paint formulations if the paints are to qualify for the voluntary Ecolabel labelling system [8]. In the future, waste management of old paint residues may also be included in the Ecolabel criteria [9].

Even before regulatory guidelines were in place, the coatings industry has strived to find a replacement for TiO_2 due to its relatively high cost compared to other coating components [10]. The recovery of TiO_2 from paint waste could benefit the coatings industry in two ways. First, recovered TiO_2 may be a cheaper and more environmentally friendly replacement for virgin TiO_2 produced by conventional high carbon footprint routes. Second, a successful TiO_2 recovery process could be a cornerstone in the waste management of old paint residues and production waste from manufacturing plants.

The aim of this work was to investigate if an inorganic TiO_2-containing residues (pigments) from waste paint can be used as a replacement, or partial replacement, for virgin pigments in paint formulations. This is based on the facts that the price of TiO_2 and the environmental impact of TiO_2 is relatively high compared to other coating components [10]. A recycling process has to be developed in order to isolate the TiO_2 pigment from other paint phases such as binders, solvents, and additives in waste paint. The necessity to separate the inorganic fraction from the organic fraction in the paint led to the choice of a

pyrolysis based process. Compared to conventional incineration it has the benefit that it breaks down the organic molecules under relatively low temperatures and in an oxygen depleted environment. The gas and the oil produced from the pyrolysis fraction could potentially be used as an energy source or as a raw material for the synthesis of chemicals, but this is outside the scope of the present work. The major shortcoming of pyrolysis is that some of the organics will be degraded into carbon black. To remove this black pigment from the inorganic pyrolysis fraction, a heat-treatment in the presence of oxygen would be needed.

1.1. Objectives

The overall objective of this work was to extract the inorganic pigment, TiO_2, from waste paint and to use it as a replacement for virgin TiO_2 pigment in new paint formulations. The work focused on white water based decorative paint. In order to recover TiO_2 from waste paint, two different heating methods for the pyrolysis process were evaluated, including microwave and conventional (conduction) heating. To be able to use the recovered pigment in the right type of products and to predict its performance in paint formulations, a thorough characterization of the recovered TiO_2 pigments was needed to investigate the effect of the recycling process on the surface properties on the pigment.

2. Background and theory

2.1. Titanium dioxide, TiO_2

The main TiO_2 producing regions are Australia and Africa, but production can be found all across the globe [11] as shown in Figure 1. The world reserve of titanium containing minerals is estimated to total more than 2 billion tons. In 2016 the mining production of rutile and ilmenite ore, the two major titanium containing minerals, was 6.6 million tons. Roughly 90% of the amount was used for pigment production in paints (60%), plastics (28%), paper (5%), and other applications (7%), such as toothpaste or as a food additive [12].

Figure 1 Titanium feedstock producers worldwide (marked in green). Adapted from [11].

There are three crystal forms of TiO_2, rutile, anatase, and brookite (see Table 1) [13]. Both anatase and rutile are relatively easy to produce, while brookite is difficult to produce and as such is not used industrially as a pigment [13, 14]. Rutile and anatase differ in how the titanium and oxygen are arranged in the crystal lattices. This gives differences in refractive indices, densities, and UV reactivity [3]. In most applications rutile is preferred to anatase due to the higher refractive index and the superior exterior durability. Anatase is preferred in special applications due to its bluer tone, its ability to function as an optical brightener, and its lower Mohr hardness, making it less abrasive [13].

Table 1 Crystallographic data for TiO_2 crystal structures [14].

Phase	Crystal system	Lattice constants [nm] a	b	c	Density [g/cm^3]
Rutile	Tetragonal	0.4594		4.21	4.21
Anatase	Tetragonal	0.3785		4.06	4.06
Brookite	Rhombic	0.9184	0.5447	0.5145	4.13

The element titanium was first discovered in 1791 by Reverend William Gregor in Cornwall England, however TiO_2 was first produced from the mineral rutile a few years later in Germany. Commercial applications of the Ti metal and the oxide were not discovered until the early 20th century. In 1916 the first TiO_2 pigment plant was built in Niagara Falls, US and in 1919 the first European TiO_2 plant was built in Fredrikstad, Norway. The first pigments produced were a mixture of anatase and barium sulphate. These pigments provided better opacity and were more compatible to the paint media than the earlier pigments based on lead or zinc [13]. The initial demand for TiO_2 pigments was still low and they were mainly considered as high priced specialty additives [11]. Early in the 1940´s, the first rutile pigments were commercially available. A few years later surface the first treatment (coatings) were applied to TiO_2 pigments, improving their dispersibility and stability [13]. In addition, lead-based pigments were then deemed to be toxic, which increased the popularity of TiO_2 pigments in the 1950's. By the mid 1970's TiO_2 pigment was the most important white pigment for paint and coatings [11]. Today TiO_2 pigment is the most important pigment in the world, accounting for approximately 70% of all pigments together [2].

While several non-pigment uses do exist, such as for self-cleaning surfaces and water or air purification [15], the most important use of TiO_2 in society is as a white pigment. TiO_2 has a high refractive index, it is chemically inert in most pigment applications, and it is only soluble in strong sulphuric or hydrofluoric acids at elevated temperatures [14]. This makes TiO_2 suitable as a pigment in most applications and it is used in a wide range of products such as paint, plastics, and paper.

2.2. Paint components

Paint formulations are usually very complex and contain many different components, but generally paint components can be divided into four major parts: binder, solvents, additives, and pigments [16]. There are different characteristics which must be considered for paint formulations, for example opacity, gloss, texture, chemical resistance, durability, resistance to mechanical wear, and adhesion to the substrate. It can be a highly challenging task to make formulations which address all the desired qualities [17] and there is a wide variety of different paint formulations.

2.2.1. Binder

The binder, also known as the film-former, is the component that normally identifies the paint, for example alkyd paint or emulsion paint. It is the part of the paint formulation that forms the dry paint film on the substrate. Without the binder holding the dry pigments in place the paint or coating would be very susceptible to wear. A varnish, which is a non-pigmented coating, still protects the surface and gives a decoration effect called gloss or "sheen". There are several types of binders, such as linseed oil, polyesters, epoxies and urethanes, of which alkyd and so called emulsion paints are the most common types in decorative paints [16, 18, 19].

2.2.2. Solvent

To facilitate the application of the paint or coating on the substrate the paint needs to be fluid. The term "solvent" is used in paint contexts to describe any liquid that is present in, or added to, a paint formulation to give the paint the correct fluidity. The term "solvent" can be somewhat misleading as it does not say anything about the ability to solve any of the paint components and the term diluent is more correct but less used. In modern decorative emulsion paints the most common solvent is water [18]. The binder-solvent mixture is also known as the paint vehicle or the vehicle for the pigment [18].

2.2.3. Additives

Paint formulations are complex mixes of inorganic and organic components and it is often found to be difficult to mix them together into a homogenous product. Therefore, additives are commonly added to a paint formulation to overcome these shortcomings and to tailor make the final product for certain applications. Examples of common additives are viscosity modifiers, anti-foaming agents, surfactants, and biocides. These are normally added in small amounts (0.001 wt.% to 5 wt.%) but have a major impact on the properties of the final product [18, 19].

2.2.4. Pigments and extender pigments

There is a vast variety of inorganic pigments, each with their own specific chemical composition, crystal structure and so forth that are used in paints and coatings. The addition of pigments to a coating formulation provides mainly two different kinds of benefits, namely decorative and protective effects [18]. Extender pigments, also known as mineral pigments, fillers, or simply extenders, have traditionally been used to dilute a more expensive product without compromising on the desired qualities. The characteristics of a extender pigment, that have no effect on the properties of the paint, are that it should reduce the total cost of the whole product, be chemically inert, and have the correct particle size. However, nowadays almost all extender pigments can be seen as functional fillers with their own purpose and function in a coating formulation. They are still used to add bulk to the system for financial gain, but the choice of extender pigment is based on its physical and chemical characteristics and how it will affect the whole coating system [13]. The functions of the extender pigment could be to improve durability and strength or to reduce gloss of a paint film [18]. What distinguishes an extender pigment from a traditional pigment is the function, as the latter is mainly used as a colourant [14].

The carbonates are probably the most widely used extender pigment based on weight consumed. This group contains minerals such as white crystalline limestone, marble, aragonite and dolomite. The major advantage of carbonates is their abundance. However, the carbonates can be replaced with another extender pigment that is more abundant in a certain area or with an extender pigment more suitable from a technical aspect giving large variations in coating formulations.

Common replacements for carbonates are kaolin (kaolinite) and talc [13]. There are also synthetically produced extender pigments that have the advantages of having a narrower particle size distribution and higher chemical purity. Examples of synthetic extenders are synthetic calcite or aragonite crystals called precipitated calcium carbonate (PCC) and a barium sulphate called blanc fixe [13, 20]. White decorative paint is the focus of this work which is why organic and inorganic coloured pigments will not be discussed.

2.3. TiO_2 pigment properties

The most important quality of a white pigment in a paint is its ability to provide a white colour with enough opacity to cover the substrate it is applied on. However, the pigment can also effect properties such as gloss and durability of the final paint film [13] and the rheology of the wet paint [21]. These properties are all functions of chemical purity, crystal structure, particle size distribution, and the coating on the TiO_2 pigments. However, it must be mentioned that the effect of the TiO_2 pigment on the paint is also dependent on the paint matrix and also these correlations cannot often be accurately described or predicted [14].

2.3.1. Opacity

The opacity of paint is defined as the ability to hide the painted substrate. To hide the substrate, the pigment has to prevent light from passing through the paint film, reaching the substrate and bouncing back to the observer's eye. The ability of a pigment to obliterate the substrate is dependent on its ability to either scatter or absorb light [22]. Coloured pigments absorb the incoming light while white pigments scatter the light. In most cases a combination of scattering and absorbing pigments gives the best opacity [17]. The absorbing and scattering capability of a pigment depends on the wavelength of the incoming light, on the pigment's crystal structure, the refractive index, and the particle shape and size [22].

A larger difference in refractive index between the continuous media and the pigment particle itself gives higher opacity [13]. Extender pigments, such as calcium carbonates and clay minerals typically have refractive indices in the range of 1.4 - 1.6. As is shown in Table 2 this is very similar to the refractive index of the binders, thus extender pigments provide very little opacity by themselves. White pigments with refractive indices of 2.0 - 2.7 are used to improve the hiding power of coatings. TiO_2 is the main white pigment due to its high refractive index and its low absorption of light in the visible spectrum. Thus, white paints with high opacity can be made of paints based on TiO_2 [17].

Table 2 Refractive indices of some common paint components [17].

Media	Refractive index	Pigment/Extender	Refractive index
Air	1.00	Calcium carbonate	1.58
		Kaolin/China clay	1.56
		Talc	1.55
Water	1.33	Baryte (barium sulphate)	1.64
		Zinc oxide	2.01
		Zinc sulphate	2.37
Film formers/ binders	1.4 - 1.6	Anatase	2.55
		Rutile	2.76

The particle size and the distribution of the pigments in the paint film are also important to reach optimum opacity. The ability of a pigment to scatter light increases with particle size until it reaches a maximum, then the scattering ability decreases as the particle size continues to increase. As a guideline, the particle size should be half the wavelength it should be able to scatter. Visible light has a wavelength of 360 nm to 780 nm so the optimum particle size for pigments is about 200 - 300 nm [22]. The mean crystal size is controlled during the manufacturing of the pigment, but the final particle size in the application is also influenced by the dispersion process when the pigment is incorporated into the paint matrix [13].

2.3.2. Colour

There are two important concepts regarding the colour of TiO_2 pigment. The first is whiteness or brightness, which is mainly how white the paint gets with the used TiO_2 quality. The second is undertone which is of importance when white pigments are used in mixtures with coloured pigments to produce specific colours [13].

The colour is governed by the crystal structure, the chemical purity, and to a lesser degree for pure white systems, the particle size of the pigment. Chemical purity is most important for high whiteness, especially the absence of transition metals, such as iron, chromium, vanadium and compounds thereof [3]. TiO_2 in the rutile form is not perfectly white since it absorbs some of the light in the 400 - 500 nm range, thus giving more cream-toned whites [13]. The anatase form absorbs less in this region, giving it a slightly bluer tone. The particle size also affects the colour as smaller TiO_2 particles scatter light of shorter wavelengths more strongly than larger particles. Thus, smaller particles have a slightly bluer tone while larger particles has a more yellow tone [14].

2.3.3. Durability

The concept of durability regarding TiO_2 pigments is not normally the durability of the pigment itself, rather it is the durability of the paint. Both anatase and rutile absorb ultraviolet light. This energy mainly dissipates as heat but can give rise to electronically excited species on the pigment surface, and they can oxidize organic molecules absorbed on, or close to, the pigment [23]. When TiO_2 pigment adsorbs ultra violet light, electrons are excited from the valence band to the conduction band, generating positive holes and free electrons which are free to move within the crystal lattice and recombine. In the presence of water or oxygen at the surface of the crystal, the holes and free electrons can take part in redox reactions which result in hydroxyl and perhydroxy radicals according to [13]

$$TiO_2 + h\nu \rightarrow e^- + \text{hole}^+ \qquad \text{Eq. 1}$$

$$\text{hole}^+ + OH^- \rightarrow OH^\bullet \qquad \text{Eq. 2}$$

$$e^- + O_2 \rightarrow O_2^- \qquad \text{Eq. 3}$$

$$O_2^- + H_2O \rightarrow OH^- + HO_2^\bullet \qquad \text{Eq. 4}$$

These radicals can then initiate the degradation of the organic binder of the paint, causing loss of gloss and chalking [13]. The surface of an anatase particle is 10 times more reactive than the same surface of a rutile particle and it only takes 10 percent contamination of anatase in rutile to reduce the life expectancy of a polymer in a paint film by half [3]. The high photo activity of anatase makes it unusable in exterior applications and it was not until the late 1940's, when the surface treated rutile grades reached the market, that TiO_2 could be used successfully outdoors. Untreated rutile can absorb ultraviolet light and even if this protects the deeper layers of the paint film, the photo-catalysed oxidation of the paint film will contribute to the rapid degradation of the surface of the film [23].

The photo activity of the pigments is reduced by incorporating stabilizing elements, such as zinc or aluminium which in the rutile crystal lattice act as recombining sites for the holes and electrons. Another approach is to coat the rutile crystals with hydrous oxides of silicon, aluminium, or zirconium [13] which act as a barriers, hindering the radical species to transfer from the pigment crystal to the organic component of the paint [6].

2.3.4. Gloss

Gloss is not a purely physical quantity, it is also dependent on physiological and psychological factors [14]. It is the sensation experienced by an observer when light is reflected from an object [13]. A high gloss surface reflects more of the incident light at the specular angle than a less glossy surface. This requires a smooth surface as a rougher surface reflects the light at all angles [24]. Surface irregularities larger than about a micrometre are large enough to decrease the gloss significantly [13]. Normally, highly pigmented paints have low gloss as pigment particles that extend through the surface and reduce the smoothness of the paint film [24].

TiO_2 pigments are used in paints to give opacity to the paint film. An increased concentration of TiO_2 increases the level of opacity. Unfortunately this can also cause the gloss to decrease. Larger particles decrease the gloss more than smaller particles. Thus, the presence of flocculated pigment particles gives a decrease in gloss compared to pigments that are well dispersed in the paint matrix [13].

2.3.5. Dispersibility

Pigments are grown into a suitable crystal size during the production process [3]. However, as pigments tend to form aggregates during transport and storage the primary objective during paint manufacturing is to break up these pigment aggregates and incorporate them into a paint matrix as uniform and stable particle dispersion [3, 4]. Dispersion (also referred to as grinding of pigment) is the process where pigments are incorporated and uniformly distributed into the liquid medium of the paint [4, 6]. The ease by which this is done refers to the dispersibility of the pigment.

The first step of the dispersing process is wetting, where gases (normally air) and contaminants are removed from the pigment surface and replaced with the paint vehicle [3]. Thereafter pigment aggregates are broken down by applying mechanical force [6]. The wetting is dependent on factors such as the nature of the liquid phase, the chemical character of the solid surface, the dimensions of the clusters and the type of the mechanical processes used to disperse the system [25]. In a practical application, surfactants are used to adjust the surface tension of the liquid and the solid-liquid interfacial tension to enhance wetting [26]. These surfactants can be of ionic or non-ionic type and are added to diffuse quickly to the solid/liquid interface, displacing air between the particles or in any capillaries in the particles [26]. Uncoated TiO_2 pigments are very cohesive which can make agglomerates hard to break [6]. By coating the pigments, the cohesive forces can be reduced. An organic coating can also be used depending on application to make the pigment easier to wet by the paint vehicle [26]. The wetting of TiO_2 pigment particles has been studied in detail by Abrahao et al. [27].

There is always some flocculation of pigments in a paint system. Even for a well-milled paint it has been estimated that only 20 - 25% of the TiO_2 particles exist as single units [13]. However, the dispersion must be stabilized to hinder further aggregation over time. Typical paint formulations are normally not stable from a thermodynamic viewpoint. The goal is to make them kinetically stable so they have a reasonable shelf life acceptable for the customer.

There are three main mechanisms that hinder dispersed particles from agglomerating. The first mechanism is electrostatic stabilization, in which the local increase in the counter ion concentration between two particles approaching each other leads to an influx of water to decrease this high local ion concentration and this, in its turn, leads to the separation of the particles stabilizing the dispersion. In the second mechanism, steric stabilization, polymer chains are firmly attached to the particle surface, and polymer segments "sticking out" from the particle surface increase in local concentration, as particles approach each other. This leads to an increase in osmotic pressure leading to an influx of water, which separates the particles from each other, leading to a stabilization of the dispersion. The last mechanism is electrosteric stabilization, which is a combination of the first two mechanisms. The particles' charge is of major importance for particles stabilized by means of electrostatic interactions, but the charge can also be very important for the adsorption of ionic polymers on to the particle surface [28].

2.3.5.1. DLVO theory

The well-known Derjaguin- Landau Verwey-Overbeek (DLVO) [29, 30] theory is commonly used to understand the stability of colloidal systems. Paints are, in general, complex mixtures of many surface active components with high particle concentrations, which are hard to accurately describe on a theoretical level. However, from literature these theories have been shown to serve well as guidelines for practical applications [25] and the DLVO theory has previously been applied on paint formulations [31].

The most important attraction force between colloidal particles is normally considered the van der Waals interactions. This is an attractive electrical force of molecular origin which is the result of three types of interactions: dipole-dipole interaction (Keesom force), dipole-induced dipole interaction (Debye force) and induced dipole-induced dipole (London dispersion force). Of these, the London dispersion force is the most important and it arises from fluctuations in the electron density distribution [26]. For homogenous colloidal particles, with radius a, that are made up of a cluster of atoms, the attractive potential between two spheres at a distance S_0 can, with $S_0 << a$, be expressed as [26, 32]

$$\Phi_A = -\frac{A_{121} a}{12 S_0} \qquad \text{Eq. 5}$$

where A_{121} is the effective Hamaker constant of two identical particles with Hamaker constant A_{11} in a medium with Hamaker constant A_{22} [26]. The Hamaker constant represents the pairwise summation of the van der Waals interactions acting between all molecules in one particle with those in the other particle [32]. Due to Brownian movements, dispersed pigments particles continuously collide. The particles will agglomerate over time if there is no counter force to balance the attractive forces [33].

Almost all oxide materials are hydroxylated when in contact with moisture. The reason for this is mainly that surface oxygens have lower coordination and are more reactive than those in the bulk, therefore the dissociative adsorption of water will reduce the surface energy [34]. In an aqueous system these surface hydroxyls can de-/protonate according to

$$\equiv M-OH_2^+ \overset{K_1}{\rightleftarrows} \equiv M-OH \overset{K_2}{\rightleftarrows} \equiv M-O^- \qquad \text{Eq. 6}$$

at different pH-values [32]. The charged sites on the oxide surface give rise to a surface charge [35]. The surface charge is compensated by counter ions (opposite in charge to the surface) and co-ions (same sign as the surface). There are several different models that attempt to describe the distribution of the ions close to a charge surface [35]. In the Stern-Grahame model, the region closest to the surface is represented by a non-diffuse part (Stern layer). There are two types of ions in the Stern layer, physically adsorbed counter ions (outer Helmholtz plane), and chemically adsorbed ions which lose part of their hydration shell (inner Helmholtz plane) [26]. Outside the Stern layer the diffuse layer is formed, consisting of counter ions that are attracted to the surface but repelled by the Stern layer. Together the three layers, the charged sites on the surface, the Stern layer of firmly attached counter ions and the diffuse layer, form the so-called electric double layer [35]. The uneven distribution of charges results in an electric potential that decays exponentially with the distance to the surface until it reaches that of the bulk liquid [26] which is shown schematically in Figure 2.

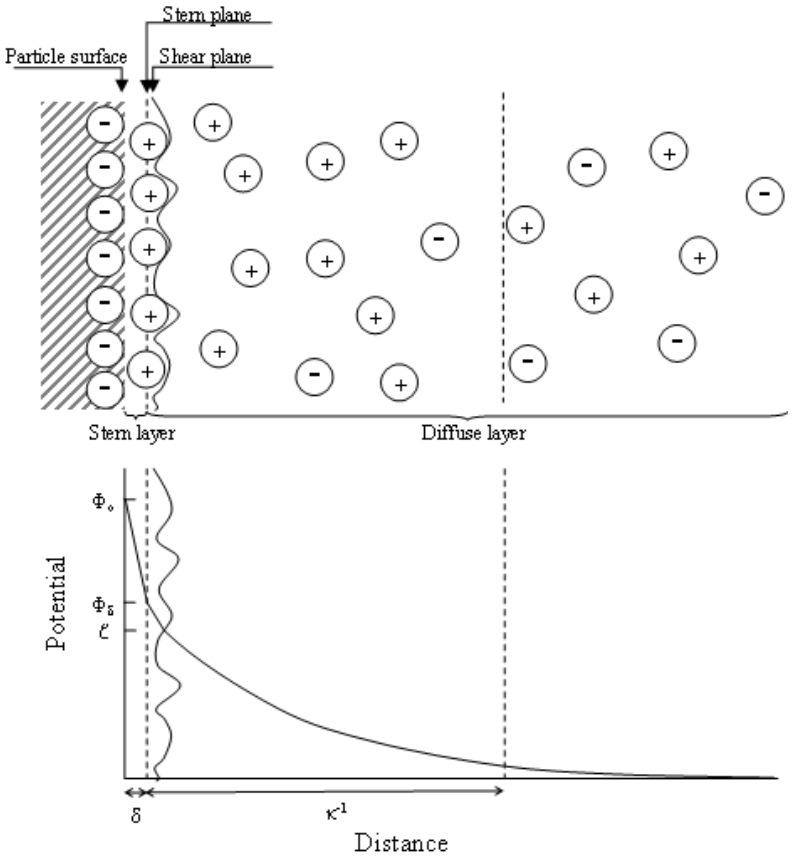

Figure 2 Schematic representation of the double layer according to Stern and Graham, adapted from [36]. The thickness of the Stern layer is given by δ. The diffuse layer starts at δ and extends roughly by the Debye length, κ^{-1}. The potential measured electrophoretically is the so-called zeta potential.

An important concept regarding the double layer is [32]

$$\kappa = \sqrt{\frac{\sum_i e^2 z_i^2 n_{i,\infty}}{\varepsilon \varepsilon_0 k_B T}} \qquad \text{Eq. 7}$$

which is the Debye screening parameter where index i stands for an ion in solution, n_∞ is the ion concentration in the bulk, z is the valence of ion, ε and ε_0 are the permittivity in the liquid and vacuum, respectively. The inverse Debye screening parameter is the so-called Debye length which is referred to as the thickness of the double layer and it strongly depends on the concentration and the valence of ions in solution [32].

When two charged particles approach each other, their double layers start to overlap. The potential between the two particles is no longer zero as it would be if $S_0 \to \infty$. The accumulation of ions between the particles leads to a repulsive potential (entropic effect) [26, 32]. The repulsive potential between equally sized sphere particles represented by an electrostatic repulsion given by [32]

$$\Phi_R = \frac{64\pi a n_\infty k T Z^2}{\kappa^2} e^{-\kappa S_0} \qquad \text{Eq. 8}$$

and

$$Z = \tanh\left(\frac{ze\psi_\delta}{4kT}\right) \qquad \text{Eq. 9}$$

where ψ_δ is the Stern potential.

The summation of the van der Waals attractive potential, Φ_A, and the electrostatic repulsion, Φ_R, of the electrical double layer, results in a net interaction potential [32]

$$\Phi_{net} = \Phi_A + \Phi_R \qquad \text{Eq. 10}$$

that is commonly referred to as the DLVO theory [29, 30]. The stability of a colloidal suspension can be described by this net interaction potential [32]. A schematic plot of the total interaction potential for a pair of spherical particles as a function of S_0 (distance) is shown in Figure 3. At very short separation distances, a deep primary energy minimum exists which results in aggregated particles. At intermediate distances, a potential energy barrier, Φ_m, forms which prevents aggregation [32]. In some cases, especially for large asymmetric particles, flocculation can occur in the secondary energy minima. This flocculation can be beneficial as it can, for example, prevent hard sediments [26].

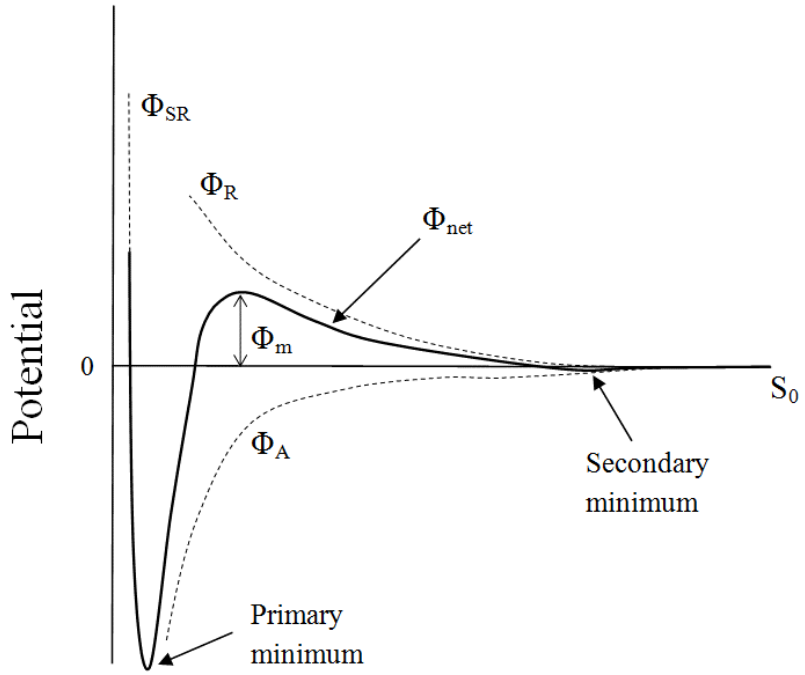

Figure 3 Schematic presentation of the DVLO theory as a function of particle distance, S_0. Φ_{net} is the net interaction potential for a pair of spheres, Φ_A is the van der Waals attractive forces and Φ_R the electrostatic repulsion. Φ_{SR} is shorted ranged repulsion which is not a part of the DVLO theory itself [32].

Combining Eq. 5, Eq. 8, Eq. 9, and Eq. 10 yields

$$\Phi_{net} = -\frac{A_{121}a}{12S_0} + \frac{64\pi a n_\infty kTZ^2}{\kappa^2}\tanh^2\left(\frac{ze\psi_\delta}{4kT}\right)e^{-\kappa S_0} \qquad \text{Eq. 11}$$

It can be seen that the Hamaker constant A_{121}, the Stern potential ψ_δ and the Debye screening parameter, κ, all are important to the shape of the DLVO curve and the magnitude of the potential barrier that prevents aggregation. Larger Hamaker constant yields lower barriers, thus aggregation is more likely. A larger magnitude of the Stern potential gives a larger electrostatic barrier which prevents aggregation. Finally, in Eq. 7 can it be seen that Debye screening parameter, thus the electrostatic repulsion, is strongly dependent on the salt concentration n_∞ and the valance z of ions in solution. A high salt concentration can in practice remove the electrostatic repulsion between particles [32] and cause aggregation of particles.

2.3.6. Coatings and surface properties

Commercial pigments are designed to meet specific requirements for specific customers. Commercial pigment grade TiO_2 is often not 100% pure. The crystalline, TiO_2 core is the active ingredient that provides the optical functions. As the TiO_2 crystals grow during manufacturing, insoluble components accumulate on their surfaces. These components are either impurities from the ore or additives deliberately used to control crystal structure, crystal growth, or coatings on the particle surface. The layers of these "non-TiO_2" molecules could be only a few molecules thick [3, 4]. Most surface treatment methods and additives used are well-guarded manufacturing secrets [3]. However, the most commonly used coatings are oxides, oxide hydrates, silicates, and/or phosphates of titanium, zirconium, silicon, and aluminium [14]. The pigment can also be treated with an organic coating. The pigment can be made either more hydrophobic, with compounds such as silicones, or more hydrophilic with the use of alcohols, esters, or ethers [14]. It is also common that the pigments are treated with organic polyhydroxyl compounds to improve their dry flow characteristics [3].

Pigments are coated for two main reasons: (1) to reduce the photo activity which improves the life-time of the final paint film and (2) to improve the dispersibility of the pigment into the paint matrix [14]. The knowledge of the DVLO theory can be applied to the dispersibility and the stability of TiO_2 pigments. As shown in Table 3, rutile has a relatively high Hamaker constant. Coating the rutile pigment with silica or alumina reduces the Hamaker constant, thus reducing the attractive forces between pigment particles and improving the colloidal stability [21]. The thickness of the coating should be at least 2 nm to have an effect [37].

Table 3 Hamaker constant [38] and IEP [39, 40] for given compounds in water.

Compound	Hamaker constant [10^{-21} J]	IEP
Alumina	21-67	7.6-9.3
Silica	1.6-8.4	1.3-3.8
Rutile	60-94	3.4-6.0

As shown in Eq. 11, a high Stern potential, ψ_δ, is beneficial for an electrostatically stabilized system. So far, it has not been experimentally possible to measure the Stern potential directly, but it can be estimated by, for example using, an electroacoustic technique where an oscillatory electric field is applied to a colloidal suspension. These oscillations induce a displacement between the charged core particle and the surrounding ions in the diffuse layer, giving rise to an acoustic response to the applied alternating electric field. The sound wave created can be correlated to the movement of charged particles in the external electric field [41, 42]. The movement of charged particles induced by the external field displaces the ions from the outer part of the diffuse layer, the so called shear or slip plane of the electric double layer. The potential at this shear plane can be calculated and this is the so called zeta potential (ζ-potential). The exact position of the slip plane within the double layer is not sharply defined but it is assumed to closely correspond to the potential at the boundary between the Stern layer and the diffuse layer, as presented schematically in Figure 2.

Information about the zeta potential can be helpful in practical applications such as predicting dispersion stability and agglomeration [43, 44]. For electrically stabilized suspensions, a larger magnitude of the zeta potential results in a more stable suspension. For a given system the zeta potential is strongly dependent on pH as the surface hydroxyl groups on the dispersed particles de-/protonate according to Eq. 6. The conditions at which the zeta potential equals zero is called the isoelectric point (IEP) [32]. At a pH below the IEP, more of the surface hydroxyls are protonated, giving a more positive zeta potential, and at a pH above the IEP more of the surface hydroxyls are deprotonated which gives a more negative zeta potential [45]. The magnitude of the charge is normally larger the further the pH is from the IEP and is illustrated for different oxides in Figure 4. Thus, the magnitude of the surface potential is highly dependent on the acid/base characteristics and the concentration of the surface hydroxyl groups (governed by the type of oxide) and the pH [32].

By coating a rutile pigment with a different oxide, not only does the Hamaker constant change, the surface charge, thus the electrical repulsion, of the pigment is also altered. The IEP for silica tends to be at a lower pH while the IEP for alumina tends to be at a higher pH when compared to rutile as shown in Table 3. Thus, by modifying the composition of the surface coating the surface charge of the pigment particles be can altered. A layer of silica would provide the surface of the pigment with a more negative charge at the alkaline pH of a typical water based decorative paint [31]. However, TiO_2 pigments are normally treated with alumina as the pure TiO_2 surface provides poor anchoring sites for the anionic dispersant molecules commonly used in paint formulations. A slurry made from uncoated pigments can still be used, as the dispersant molecules will still anchor to the surface, although with weak interactions. When an uncoated pigment is mixed with other pigments and/or resin molecules which have stronger anchoring sites for the dispersant molecules, the TiO_2 surfaces are stripped of the dispersant molecules leading to flocculation of the TiO_2 pigment. Alumina has strong anchoring sites for dispersants and by adding a coating of alumina to the TiO_2 particle, the tendency of the dispersant to be stripped from the surface will be decreased [46].

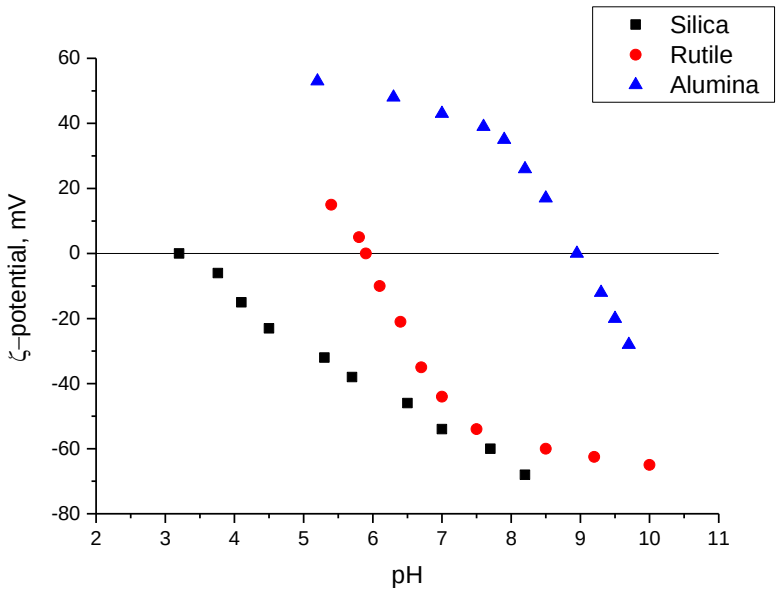

Figure 4 Illustration how magnitude of the zeta potential can vary with pH for silica, rutile and alumina. Data taken from literature [47, 48].

2.4. Paint waste and recycling

The annual worldwide production of decorative paint is estimated to be 3.1 billion litres. Of this approximately 50% goes to professionals and 50% to do it yourself (DIY). Professional painters do not normally waste any paint while DIY's waste up to 25% (Akzo Nobel Decorative Paints, personal communication, 12 January 2018). In Scandinavia one of the largest source of hazardous waste from households is waste paint. The packaging is normally recovered while the waste paint is incinerated at high temperatures [49, 50]. The ash from incineration is then landfilled.

The soundest approach to the reduction of this waste stream would be to use less hazardous components in paint formulations or to reduce the DIY paint consumption. However, already today much of the water based paint on the market is not necessarily classified as hazardous waste [50, 51] but it can be hard to sort hazardous paints from non-hazardous paints [51]. To simplify the handling of paint waste, it is easier to classify it as hazardous if there is any doubt. The voluntary Ecolabel labelling [8] includes criteria regarding both the toxicity of paint components and demands regarding the quality of paints which in the end would reduce the consumption of paint. There are also initiatives where the old paint is reused, either directly or as a component in new batches of paint. Left over paint is collected, processed, and products based on recycled paint are today sold to individuals [52]. One such initiative is the Community Repaint organisation in the United Kingdom that is collecting and distributing usable waste paint to people and organisations needing paint. In 2013 this organisation transferred over 245 000 litres of paint to community groups, charities, voluntary organisations and people in social need [53]. However, this option is not always applicable due to dry non dispersible paint lumps, incompatible paint components, microbiological contamination and the changing chemical and biocide regulations that would make the new paint unusable from a legal perspective.

This would leave the option of recycling the paint waste where valuable materials are extracted from the paint waste. There are a handful of publications found in the literature dealing with the recycling of paint components. The majority focus on industrial paint waste (sludge) from paint cabins used in some kind of production facility. The probable reasons for this focus is that the paint waste is relatively homogenous and complicated logistics of collection waste paint in large volumes are avoided. There are a few publications based on the idea that the organics in the paint is the valuable component and for example pyrolysis is used to reduce the amount of waste [54] and turn organic component into fuel [55], or into activated carbon for use as absorbent [56]. There are also publications that focus on the inorganic fraction of the paint and describe attempts to recycle it as composites as additives for metal or plastic production [57]. Finally, there have also been suggestions to use paint waste to produce for example sealants [58], asphalt, cement, concrete, mortar, and plaster [59].

There are very few publications that describe processes where the waste paint components are recovered and used in new paints. Sanghvi and Massingill [60] treated paint sludge in a low temperature vacuum process and used the solid residue in new paint formulations while Seyed et al. [61] extracted TiO_2 from paint sludge and used it in new paint. Neither of these publications describe any detailed investigations into the effect of the recycling process on the TiO_2 pigment.

Since paint contains both inorganic and organic components, a recycling process must separate these components. For white decorative paints the binder and the additives can mainly be classified as organics, while the pigments are inorganics. The solvent can either be an organic solvent or water, which is most commonly used today. Pyrolysis can be used to separate the organic fraction from the inorganic fractions. The temperature in the process must be high enough to decompose the organics but not too high as to effect the inorganic pigments. At high temperatures, the inorganics either degrade or react with each other, creating new chemical species. Another issue with TiO_2 recycling is that the inorganic fraction after the pyrolysis will contain many other components, other than TiO_2.

Table 4 lists some of the different inorganic components that can be found in a paint waste stream consisting of white decorative paint. A recycled TiO_2 fraction containing these extender pigments would most likely give a reduction of whiteness and gloss to the paint formulation they are used in.

Table 4 Different kinds of extenders that are used in paint and coatings [13, 20] (Note: chemical compositions given are only theoretical. Most extenders come from natural minerals and contain minor impurities).

Extender	Mineral example	Theoretical composition
Carbonates	Calcite, Aragonite, Dolomite	$CaCO_3$, $MgCO_3$ or $CaMg(CO_3)_2$
Kaolin	Kaolinite	$Al_2O_3 \cdot 2SiO_2 \cdot 2H_2O$
Talc		$Mg_6[Si_8O_{20}](OH)_4$
Silica	Perlite, Diatomite, Tripoli, Novaculite	SiO_2
Barytes		$BaSO_4$
Nepheline		$K_2O \cdot 3Na_2O \cdot 4.5Al_2O_3 \cdot 20SiO_2$
Mica	Muscovite	$Al_3KSi_3H_2O_{12}$
Wallastonite		$CaSiO_3$

2.5. Pyrolysis

The word pyrolysis consists of the two Latin words Pyro meaning fire or heat, and Lysis meaning decomposition or disintegration. A pyrolysis process can be described as the chemical decomposition of organic substances by elevated temperature and in an oxygen free environment. Pyrolysis is also known as carbonization, destructive distillation, dry distillation, or retorting.

Pyrolysis is a thermal process for the degradation of organic materials in the absence of air into carbonaceous char, oils and combustible gases at a relatively low temperature (400 - 800 ^oC). The major differences between combustion and pyrolysis are the heat generation/demand and the products of the processes. Combustion is an exothermic reaction while pyrolysis is endothermic. The combustion products are carbon dioxide, water and ash while a pyrolysis process generates char, oil, or tar in addition to various gases [62, 63].

By adjusting the heating rate and the maximum temperature, the ratio between char, oil, and gas can be modified [63]. Faster heating and higher maximum temperatures generally produce higher ratios of oil and gas compared to char, and as the residence time in the furnace increases, the yield of the liquid phase decreases and more gas is produced [63, 64]. The chemical composition of the oil is dependent on the feedstock and the process parameters. The gas phase mainly consists of carbon dioxide, carbon monoxide, hydrogen, methane and other hydrocarbon gases, and uncondensed pyrolysis oils [63]. Both the oil and the gas can potentially be utilised as fuels or as feedstock for chemical syntheses.

The heating can be provided using conventional methods, for example internal (by partial combustion of fuel) or by external heat sources of the reaction or electrical resistance, or by microwave heating. Microwave induced pyrolysis of a number of waste types, such as sewage sludge [65], car tires [64], and plastic wastes [66] has been described in literature. Differences between conventional and microwave heating are presented in Table 5.

Table 5 Differences between conventional and microwave heating [64].

Conventional heating	Microwave heating
Long reaction time (hours)	Short reaction time (minutes)
Slow transfer of heat, thermal conductivity of polymer is low	Easier heating of polymers
Low heating efficiency	High heating efficiency
Every fuel source may be employed	Electrical power is required
Additive not required	Microwave absorber is required

Compared to conventional heating with an external heat source the heat generated by microwaves is generated volumetrically within the exposed material. This gives the potential of a very uniform heating process. But this requires a uniform material, as different materials absorb microwaves differently [67]. A material can either be transparent to microwaves (low dielectric loss materials), an opaque material which reflects microwaves (no penetration) or an absorbing material (high dielectric loss) [68]. For example, carbon in the form of charcoal is very active while calcium carbonate, silica oxide, dolomite, muscovite, quartz and rutile are more or less transparent for microwaves with a frequency of 2.45 GHz, the most common frequency for industrial scale microwave heaters [69, 70].

3. Materials and methods

The aim of the study was to investigate if the inorganic TiO_2-containing residues from the pyrolysis of waste paint can be used as a replacement for virgin pigments in a paint formulation. The experimental work in this thesis is based on four publications.

In the investigation described in Paper I a model paint containing several types of inorganic pigments was pyrolysed in a pilot size microwave-heated unit, provided by Stena Metall AB. The goal of the pyrolysis process was to recover and recycle the inorganic components in the paint, mainly TiO_2. The solid residue remaining after the pyrolysis was further heat treated in air to remove the char in the TiO_2-containing product. The recovered TiO_2-containing product was used in two types of paint formulations as a replacement for virgin pigments. The properties of the paints containing recycled TiO_2 and extenders pigment were evaluated and compared with a standard paint formulation containing only virgin TiO_2 and extender pigments.

In order to be able to study the effects of the recycling process on the TiO_2 more specifically, TiO_2 was extracted by pyrolysis in an electrically heated laboratory pyrolysis oven from paints made with TiO_2 as the only inorganic pigment, as described in Papers II and III. Aluminium, zirconium, and silicon coated rutile, TiO_2 pigment were extracted from a paint matrix by means of a thermal recycling process schematically shown in Figure 5. The objective was to investigate the effect of the recycling process on the surface properties of differently coated TiO_2 pigments. The pigments were analysed using powder x-ray diffraction (XRD), surface area measurements (BET), laser diffraction for particle size analysis and X-ray photoelectron spectroscopy (XPS) before and after the recycling process. Investigations on the zeta potential were also performed.

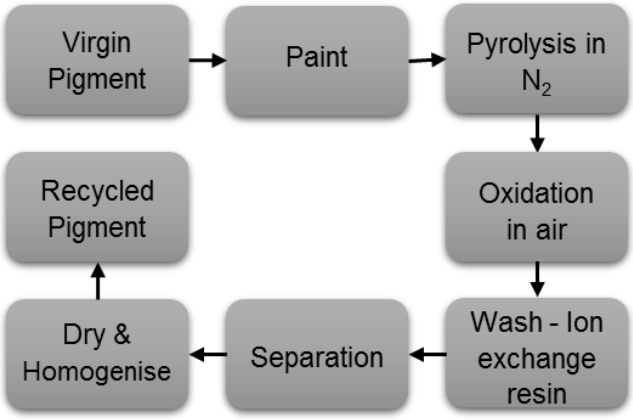

Figure 5 Schematic of the pigment recycling process used to produce recycled pigment in this work.

Finally, in Paper IV recycled TiO_2 pigment was used in a paint formulation as a replacement for pigment made from virgin raw materials. With all other pigments omitted, the evaluation of the influence of TiO_2 in the formulation is made easier. The paint was evaluated based on pH, stormer and ICI viscosities[1], gloss, hiding power and colour characteristics. The paint films were also characterised by low vacuum scanning electron microscopy (LVSEM-EDS), atomic force microscopy (AFM) and profilometry. A detailed description of the results can be found in the relevant paper but the highlights are presented in the following sections.

[1] Stormer viscosity is commonly referred to the in-can viscosity of a paint when stirring it, while ICI viscosity is referred to as a measurement of the application viscosity. More information can be found in Paint and Coating Testing Manual [80].

3.1. Recovery of TiO_2 by pyrolysis (Paper I)

3.1.1. Thermal stability of commonly used paint components

Commonly used components for white decorative water based paint were acquired from Akzo Nobel Decorative Paints, UK. The organic part of the paint was represented by two different acrylic based binders (Sample A (a vinyl acrylic latex) and Sample B (a pure acrylic latex)) while the inorganic part of the paint was represented by samples of different inorganic pigments/extenders named TiO_2, Dolomite, Kaolin, Talc and Mica. The crystalline compounds in the inorganic samples were identified with powder X-ray diffraction (XRD) using a Siemens D5000 X-ray powder diffractometer with an X-ray tube giving the characteristic Cu radiation and a scintillation detector. The 2θ range used was 10-70° with a step size of 0.050° and a 1 second step time. The identification of compounds was performed through comparison with standards in the Joint Committee of Powder Diffraction Standards [71]. The identification of a compound in a mixture is generally possible if the compound is present at a concentration of 2% by weight or more. Amorphous compounds and compounds occurring in nano-sized crystals cannot be detected by XRD.

To be able to assess a suitable temperature for a thermal recycling process for paint waste, the TiO_2 and the extenders pigments were analysed by simultaneous thermogravimetric analysis (STA) (NETZSCH STA 409 PC Luxx) which includes thermogravimetric analysis (TGA) and Differential Scanning Calorimetry (DSC). STA measures weight change as well as energy change in a sample as a function of temperature while TGA only measures weight change. The thermal stability of the binders was studied by TGA (TA Instruments Q500), however, since only weight change was measured it is not possible to say if the binders decompose into non-volatile products. Further DSC analysis would be needed for evaluation of decomposition temperatures.

Typical operating parameters for STA and TGA work are given in Table 6. A nitrogen atmosphere was used to simulate the oxygen-free atmosphere in a pyrolysis reaction. Thermolysis curves were displayed as % weight loss vs. temperature or, when needed the derivative of the thermogravimetric curve. The residues after the thermal stability analysis of the pigments were also analysed with XRD.

Table 6 Values of TGA operating parameters.

Variable	Value
Reaction temperature (°C)	100 - 1000
Balance purge rate (mL/min)	10
Sample purge rate (mL/min)	90
Sample size (mg)	10
Heating rate (°C/min)	10
Reaction gas	N_2

3.1.2. Microwave heated pyrolysis of liquid and dry paint

To assess a microwaved heated pyrolysis process two samples, Paint A and Paint B, of a white paint formulation were pyrolysed in a pilot scale microwave pyrolysis furnace provided by Stena Metall AB, Gothenburg. Paint A was a liquid paint with the composition given in Table 7 (total dry content 44 wt.%; 27 wt.% inorganic pigments), while Paint B is the same as Paint A but it was dried prior to the pyrolysis experiment to a dry content of 65 wt.%, thus containing 37 wt.% inorganic pigments. Paint B still contained some water but was non-fluid.

Table 7 Composition of the model Paint A used in the pyrolysis experiments.

Type of component	Component	Total formulation, wt.%	Pigment mixture, wt.%
Solvent	Water	32.0	
Additive	Surfactants	0.7	
	Coalescent aid	0.6	
	Biocide	0.2	
	Organic polymeric hiding additive	5.0	
	pH modifier	0.1	
	Cellulosic rheology modifier	0.7	
	Rheology modifier	0.2	
Binder	Acrylic copolymer dispersion	33.6	
Pigment	Dolomite	11.1	41.3
	Kaolin	1.2	4.5
	Talc	1.2	4.6
	Mica	1.2	4.3
	Rutile	12.1	45.2

The microwaves were produced by three magnetrons using the Samsung OM 75P model with a fixed frequency at 2465 MHz [72] and an individual power output for each magnetron of 1.5 kW. A sample container made of mica (transparent to microwaves) was used. The oven was flushed with nitrogen before each experiment. The temperature was measured continuously at three points; inside the sample, at the surface of the reaction vessel and in the gas flow out from the furnace, see Figure 6. The temperature in the sample was kept below 500 °C at all times. After the experiment the dry residues were weighed.

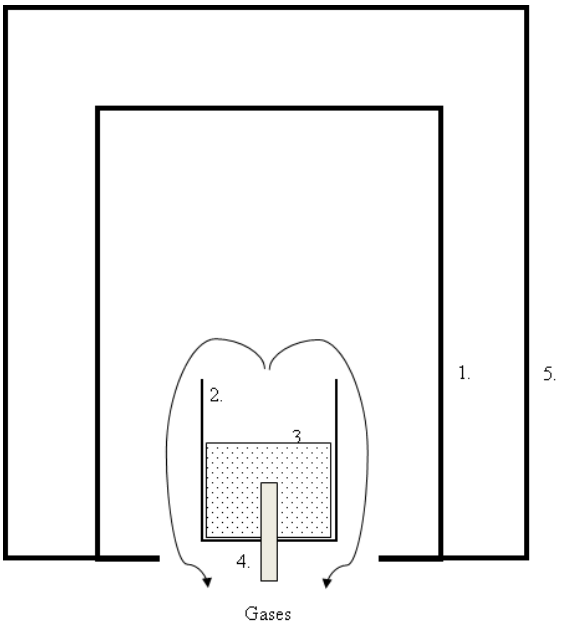

Figure 6. Schematic overview of the pyrolysis reactor used in the pyrolysis experiments.
1. Reaction vessel; 2. Sample crucible; 3. Sample; 4. Thermocouple inside sample;
5. Outer casing, continuously supplied with nitrogen gas.

3.1.3. Secondary pigment recovered via pyrolysis in paint formulations

To evaluate if the inorganic TiO_2-containing residues from pyrolysis of waste paint can be used as a replacement for virgin pigments in a paint formulation, a white paint formulation (see Table 7) was pyrolysed according to procedure described in Section 3.1.2. To remove organic residues remaining after the pyrolysis processes the inorganic pigment mixture was heat treated in air at 450 °C. After pyrolysis and oxidation the recovered pigment mixture was analysed for crystalline compounds and specific surface area using XRD (as described in 3.1.1) and The Brunauer-Emmett-Teller (BET) method [73]. The BET areas were determined by N_2 adsorption isothermal at 77 K using a Micromeritics ASAP2020. Before measurement the samples were outgassed at 60 ºC under high vacuum (roughly 1 µm Hg), until the samples were considered dry or for a maximum of 1500 minutes. The samples were considered dry when the measured pressured change due to the sample being lower than 5 µm Hg/min. The outgassing temperature has a significant effect on the BET result [74] so a relatively low outgassing temperature was chosen in order not to alter the surface of the pigment.

The recovered pigments were incorporated in two high pigment volume concentrations (PVC) formulations, shown in Table 8. To facilitate the formulation work, the pyrolysis residue was simplified as a mixture of 45.2 wt.% TiO_2 and 54.8 wt.% dolomite, as these were the major components in the residues. The TiO_2 in each formulation was substituted with the corresponding amount of recovered pigment mixture on a volume basis (ρ_{TiO2} = 4.05 g/cm^3; $\rho_{dolomite}$ = 2.85 g/cm^3) so that the volume of TiO_2 remained constant in standard paint and in the paint based on recycled material. Virgin dolomite was added when needed so that the total volume of extender pigments remained the same in the compared formulations.

Table 8 Paint formulations used (expressed in wet volume in 100 ml of paint). PVC represents pigment volume concentration.

Material	High PVC formulation 1 with virgin material	High PVC formulation 1 with pyrolysis ash	High PVC formulation 2 with virgin material	High PVC formulation 2 with pyrolysis ash
Latex binder (50% solids)	5.3	5.3	4.4	4.4
Virgin TiO_2	1.5	0.0	0.8	0.0
TiO_2/Dolomite (recycled)	0.0	4.3	0.0	2.4
Virgin Dolomite	7.4	4.6	2.1	0.5
Other virgin extenders	18.6	18.6	19.4	19.4
Additives	0.6	0.6	1.0	1.0
Water	66.6	66.6	72.3	72.3

The paints were evaluated based on the opacity, gloss, whiteness, and durability of the paint films. All values were compared to standard paint formulations based on virgin pigments. The dry paint films were also analysed using a scanning electron microscope (SEM) with energy dispersive X-ray (EDX) spectroscopic element detection (Hitachi TM 3000 with EDX, Quantax 70).

3.2. Surface properties of recovered TiO_2 (Papers II/III)

There are many different commercial pigments with diverse coatings intended for the paint industry. The waste paint feedstock going into a recycling process could therefore contain TiO_2 pigment with varied surface coatings, for example based on Al, Zr, or Si. The main purpose of this study was to understand the effects of the thermal recycling process on the surface characteristics of pigment with different surface coatings. This knowledge will help evaluate the possibility of using a thermal recycling process to recover TiO_2 pigments, and to see if certain pigment qualities are more susceptible to chemical changes during the recycling process.

Three commercially available TiO_2 pigment qualities were acquired from Akzo Nobel decorative paints Slough, UK. According to the producers of the pigments, Pigment A is a rutile pigment coated with alumina and zirconia, Pigment B is a rutile pigment coated with alumina and amorphous silica, while Pigment C is a rutile pigment coated with alumina. In order to study the effect the pyrolysis recycling process had on each of the coated TiO_2 pigments a paint was made containing TiO_2 as the only inorganic component, according to the formulation given in Table 9. A mix of inorganic pigments, although more realistically found in a paint waste stream, would make a detailed characterization of the TiO_2 after the recycling process practically impossible.

Table 9 Raw materials and theoretical properties of model paint produced for the TiO_2 recovery process.

Raw materials	**wt.%**
Mill base	
Water	22.92
Antifoam	0.51
Non-ionic surfactant	0.51
Anionic surfactant	0.46
Hydroxyethylcellulose (HEC)	0.51
TiO_2	30.47
pH modifier	0.25
Let down	
Incan preservative	0.12
Binder (vinyl acrylic)	44.25
Theoretical properties	
Volume % solids	35.5
Pigment volume concentration	26.4
Density (kg/L)	1.4

The pigment was extracted from the paint matrix through a slightly altered pyrolysis-based recycling process then the one previously discussed in Section 3.1. The pyrolysis experiments were conducted in a Rohde, ME 45-13 furnace, fitted with a pyrolysis retort in corrosion resistant steel. The inner dimensions of the pyrolysis retort were 300 x 300 x 150 cm. During the experiments, the temperature was controlled using a TC 504 temperature controller. In addition, an external thermocouple was used to monitor the furnace temperature in relation to the set temperature. Before each experiment, the retort was filled with nitrogen gas (purity 99.9 %) to an overpressure of 0.5 - 1 bar, emptied, and refilled again with nitrogen to overpressure. This was repeated three times to create an oxygen free environment. The paint was dried at 150 °C, followed by pyrolysis done under atmospheric pressure at 500 °C. During the pyrolysis experiments, the retort was flushed with nitrogen, 0.85 - 0.95 L/min. The volatilized organics and liquid produced during the pyrolysis were led out through the retort outlet. In the present work, the focus was on the inorganic components of the sample materials and therefore the oil and gas fractions were not collected for analysis.

To reduce the exposure of hazardous volatile pyrolysis products, the sample was cooled to 50 °C, under continuous nitrogen flow, in the pyrolysis retort before being removed. Once cooled, the solid residue was collected and weighed. The solid product was finally homogenized with a mortar and pestle.

The pyrolysis product mainly contained the inorganic components in the paint formulation (in this case, TiO_2) and carbon residues from pyrolysis of the organics. To remove the residual carbon and non-volatilized organic material, the pyrolysis residue was oxidized by spreading the powder in a thin layer (< 4 mm thick) in an alumina crucible, and heat treating it in 470-500 °C for 1.5 hours in air. After cooling, the material was collected, weighed, and homogenized using a M20 universal mill from IKA.

During the pyrolysis and subsequent oxidation process, the organic components of the paint were decomposed, volatized, and separated from the inorganic fraction of the paint. The inorganic fraction therefore contained pigments from the original paint but it could also contain unwanted salt residues. If in a later stage, the recycled pigments were to be re-dispersed in an aqueous system, these ionic species would dissolve and increased the ionic strength of the solution. It is known that an increased ionic strength has negative effects on colloidal stability [25] and the performance of certain dispersing aids commonly used in paints [75]. Therefore a washing of the pyrolysis product was designed.

The oxidized residue was dispersed in distilled water. Ion exchanger resin (Amberlite IR120, hydrogen form) was added to the suspension under continuous stirring and pH measurement. The amount of ion exchanger added was calculated to present an excess of exchanging sites. The pH rapidly decreased from the initial pH (> 9) to stabilize at around pH 2.5 - 3.0 after 5 minutes. After 30 minutes, the suspension was neutralized using an ionic exchanger resin (Amberlite IRN78, hydroxide form) under continuous stirring. The pH slowly increased to stabilize at around 7 after 1.5 hours. The pigment suspension with the two ionic exchangers was left under continuous stirring for 4.5 hours before being separated from the ionic exchangers through sieving. The recovered pigment was dried at 60 °C, before being homogenized into a fine powder with a mortar and pestle. At this point the product is referred to as recycled pigment.

The conductivity was measured to get an indication of the effect of the washing step. All the conductivity measurements were done with a 5-ring conductivity measuring cell calibrated with a 100 µS/cm conductivity standard from Metrohm. To this end the virgin pigment, the oxidized pyrolysis residue, and the recycled pigment were dispersed (10 wt.%) in Milli-Q water (>18.2 MΩ/cm). After 96 hours of mixing, samples of the water phases were collected, diluted with Milli-Q water and analysed with inductively coupled plasma mass spectrometry (ICP-MS, Thermo iCap Q) for cations (atomic mass ranges 7 to 238) and ion chromatography (IC, Dionex DX-100 with anion column IonPac AS-4A SC) for anions (Cl^-, PO_4^{3-}, NO_3^-).

Characterization using multiple analytical techniques was performed on both the virgin and recycled pigments to identify differences between the recycled pigments and their respective virgin reference. This was done in order to be able to assess the effect of the recycling process on the pigments. In this case a virgin pigment is referred to as a pigment used as delivered directly from the supplier. The characterization techniques used were: analysis of crystalline form of the core TiO_2 with XRD, characterization of surface species by x-ray photoelectron spectroscopy (XPS), particle size analysis, surface area determination (BET), and zeta potential measurements.

3.2.1. X-ray diffraction (XRD) and X-ray photoelectron spectroscopy (XPS)

To confirm that the main crystal structure of the rutile was intact, the virgin pigment and the recycled pigment were analysed with XRD according to the procedure described in Section 3.1.1.

The main purpose of the XPS analyses was to identify possible differences between the virgin and the recycled pigments. As stated from the pigment supplier Pigment A was aluminium and zirconium coated, Pigment B was silicon and aluminium coated, while Pigment C was aluminium coated. All pigment qualities used had a TiO_2 core. For all XPS spectra, C 1s was located at the same position and was unaltered after recycling, thus it was treated as adventitious carbon and used as a charge reference located at 284.8 eV.

It should be noted that even for TiO_2 pigments that are fully encapsulated by a coating thinner than 10 nm, it is possible to get an XPS signal of TiO_2 pigment core [21, 76]. Therefore, it was impossible to draw any conclusion regarding the patchiness or the homogeneity of the coating based on XPS data.

The virgin pigments and the recycled pigments were all analysed with XPS using a Versaprobe III from Physical Electronics equipped with monochromatic Al K_α X-ray source (1486.6 eV). The X-ray beam diameter was 100 µm and the power was 25 W. Acquisition conditions for the survey spectra (0-1100 eV) were 112 eV pass energy, 45° take off angle and 0.5 eV/step. Selected region spectra were recorded covering the Ti 2p, Al 2p, O 1s, Si2p and C 1s photoelectron peaks. The acquisition conditions were, then, 55 eV pass energy, 45° take off angle and 0.1 eV/step. Samples were mounted on a steel sample holder using double sided tape. Dual beam charge compensation was carried out by flooding the sample with low energy electrons and low energy argon ions. The element distribution in depth was estimated by depth profiling performed using Ar^+ ion sputtering with 2 kV accelerating voltage and 7 mA current. The etch rate was 5.4 nm/min calibrated on a Ta_2O_5 standard sample with a thickness of 100 nm.

3.2.2. Particle size and BET

The particle size distribution was measured by laser diffraction, using a Mastersizer MicroPlus from Malvern Instruments. The particles were measured in a dilute suspension of deionized water. Before measurement, the suspension was treated with ultrasound (200 W for 40 s applied to 30 mL of 1 wt.% suspension, using a Sonics VibraCell sonicator) to break up agglomerates. The surface area in the form of BET was measured as described in Section 3.1.1.

To study the potential aggregation of pigments during the recycling process, it would, in an optimum situation, be better to measure the particle size distribution without sonication. However, most powders show a varying degree of aggregation during storage. Thus, the use of sonication before measurement is necessary to ensure reproducible particle size data [77]. And can be seen as a benchmark, to investigate if it was possible to reach the same particle size distribution in a recycled pigment as the virgin pigment with sufficient level of dispersion.

3.2.3. Dynamic mobility and zeta potential

The zeta potential analysis was performed using a ZetaProbe from Colloidal Dynamics. The ZetaProbe operates at a field frequency range of 0.3 - 3 MHz. When the alternating field is applied, the particles (and ions) start to oscillate. As the particles move, they displace an equal volume of liquid. If the density of the particles is different from the density of the liquid, this will give rise to a sound wave. This so called Electrokinetic Sonic Amplitude (ESA) signal depends on the particle velocity and the dynamic mobility, μ_d, can be determined from this. The dynamic mobility of the particles depends on their size, their zeta potential and the frequency of the applied field.

For dilute colloidal dispersions (up to about 5 volume percent), the relationship between the ESA effect and the dynamic mobility, μ_d, of the charged particles is given by [42]

$$ESA = A(\omega)\phi\frac{\Delta\rho}{\rho_o}\mu_d \qquad \text{Eq.12}$$

where ESA is measured in (Pa/(V/cm)), A(ω) is an instrument factor, ϕ is the volume fraction of the particles and Δρ is the density difference between the particles and that of the solvent (ρ_0). The ZetaProbe measures the maximum in the pressure of the wave (Pa) per unit applied electric field strength (V/cm).

The ESA is measured at 8 different frequencies and a mobility spectrum of the sample is obtained. The zeta potential is then calculated from the dynamic mobility spectrum according to

$$\mu_D = \frac{2\varepsilon\zeta}{3\eta} G(1+f) \qquad \text{Eq. 13}$$

which is valid for spheroidal particles with thin electrical double layers [41, 78]. Here, η and ε is solvent kinematic viscosity and permittivity, respectively, and ζ is the zeta potential. Both G and *f* are complex functions. G accounts for particle inertia forces on the dynamic mobility and *f* depends on the conductance on the double layer [78].

The measuring cell contained 250 mL of sample with a stirring speed of 150 rpm. The charge of the particles was determined in a pH range from 4 to 10 by titration using a particle concentration between 1-5 wt.% in 2, 10 mM NaCl and 10 mM $NaNO_3$ (≥ 99.0% ACS regents from Merck dissolved in distilled water) using a computer controlled titrator. A particle concentration below 2.5 wt.% had a significant influence on the results, for this reason 5 wt.% was chosen for this study. The pH-electrode was calibrated daily using a 3-point calibration (pH-standards 4, 7, 10) with standards from Hamilton. The ESA signal was calibrated daily with a 0.25 S/m potassium 12-tungstosilicate hydrate standard from Colloidal Dynamics. TiO_2 with a density of 4.26 g/mL and a dielectric constant of 40 and the properties for water at 20 °C were chosen for calculating the zeta potential. 1 M HCl and 1M HNO_3 was used for titration of samples dispersed in NaCl and $NaNO_3$, respectively. For both electrolytes 1 M NaOH was used as base. All bases and acids were prepared from Titrasol concentrates (Merck). All data presented was corrected for the signal from the background electrolyte, although not corrected for change in pH. The influence of pH was checked, and the signal contribution was less than 2 % except when approaching a pH of 2, where the influence could be up to 10 % of the total ESA signal. As titration was done in pH 4 to 10 this contribution was neglected.

3.3. Characterization of paints formulated using recovered TiO_2 (Paper IV)

To evaluate the performance of the recycled pigment in a real application, it was incorporated into the paint formulation given in Table 9. This formulation represents a general emulsion paint, with the main difference to a normal paint formulation being that it excludes all pigments other than TiO_2. With all other pigments omitted, the evaluation of the influence of TiO_2 in the formulation is made easier. All materials used in the paint fabrication, except the recycled TiO_2 pigment, were of commercial quality and used as acquired from Akzo Nobel Decorative Paints, UK and Akzo Nobel Performance Additives, SE.

The pigment used for this study is Pigment C that was recycled and characterized as described in Section 3.2. A summary of the pigment properties is given in Table 10. The properties of the paint based on recycled pigment were compared to the properties of a standard paint with the same formulation but based on virgin pigment. To homogenise the recycled pigment before use the pigment was milled with a ball mill (RJM 103 from EnviSense (PL)). Approximately 350 g of recycled pigment (roughly 80 mL) was placed in a 1 L LDPE bottle (outer diameter: 95 mm; height: 206 mm) with 65 stainless steel balls (8 mm in diameter). The pigment was milled at 300 rpm for 2 h.

Table 10 Properties of pigments used to produce paints for evaluation (adapted from [paper II]).

Pigment	Type	Coating	Conductivity (10 wt.%)	Specific surface	Particle size			Isoelectric point (in 10 mM NaCl)
					D(v,0.1)	D(v,0.5)	D(v,0.9)	
Virgin pigment	Rutile	Al	0.2 ± 0.1 mS/cm	17 m^2/g	0.15μm	0.28 μm	0.43 μm	7.4
Recycled pigment	Rutile	Al	< 0.001 mS/cm	16 m^2/g	0.13 μm	0.27 μm	0.45 μm	7.6

The paint was produced with a high-speed impeller dispenser from Dispermill Vango 100 from ATP Engineering (NL) with a dissolver blade of 50 mm in diameter. The mill base was dispersed at 2000-2500 rpm (peripheral speed of 300-400 m/min) for 15 min. The geometry of the dispersing vessel and position of the dispenser blade was according to guidelines given by Patton [79].

Properties evaluated on the liquid paints were pH and viscosity in the form of Stormer and ICI viscosity, while the hiding power, gloss, and colour characteristics were measured on dry paint films. All properties were evaluated using test methods adopted from the standard methods commonly used by the paint industry. General information regarding the test methods can be found in [80] while specific details to methods are given in 3.1.1and 3.1.2. The dry paint films were also analysed by atomic force spectroscopy (AFM), and Low Vacuum Scanning Electron Microscopy with Energy Dispersive Spectroscopy (LVSEM-EDS), and profilometry.

3.3.1. Test methods used on liquid paints

Stormer viscosity was measured in Krebs Units (KU) at room temperature with a Krebs Units viscometer (Braive instruments). ICI viscosity was measured in poise (P) using a CAP1000 + viscometer (CIAB instruments) at 25 °C with spindle number 01 at 750 rpm. The pH was measured with a LE 409 pH electrode connected to a FE20 pH meter (Mettler Toledo). The electrode was calibrated daily using a 3 point calibration curve with pH standards 4, 7, and 9 (Labservice AB). Stormer viscosity, ICI viscosity and pH were all measured 24 h after paint manufacturing.

To evaluate shelf life, the paints were stored at 50 °C for 5 weeks. After cooling to room temperature, the Stormer viscosity and ICI viscosity were measured. An ocular inspection was also made of the stored samples to identify any signs of syneresis (liquid/liquid separation) or settling.

3.3.2. Test methods used on dry paint films

Before applications were made for paint film evaluation, the paint samples were filtered through a 125 μm filter to remove possible residual agglomerates or dry paint film. Drawdowns of 150 μm wet film thickness at a speed of 1500 mm/s were made with an Automatic Film Applicator L (BYK instruments) on black and white (Form 10B) checkerboard charts (Leneta Company). The paint films were stored at room temperature to dry and the colour characteristics, hiding power and gloss were then analysed.

Colour characteristics were measured with a CM-600 handheld spectrophotometer (Konica Minolta) in the L*,a*, b* colour space [81] with Illuminant D65. The colour difference between paint based on virgin and recycled pigment is expressed as ΔE^*_{2000} where the virgin pigment is used as the reference [82]. The hiding power of the paint films was measured, as the ratio of the reflective tristumulus Y (CIE) over the black and white part of the Leneta chart, using a chroma meter (Konica Minolta CR-300). Both colorimeters used were calibrated to substrates with known colour coordinates. The gloss of the dry paint films were measured at angles 20°, 60°, and 85° with a micro-TRI-gloss (BYK Gardner). Before each measurement, the instrument was calibrated against the integrated standard that comes with the instrument. In addition to the drawdowns, the paints were also applied with a roller (Elite rollerset, Anza) for wall and ceiling applications, on a black Leneta sheet. Both paints were applied with a calculated wet film thickness of 200 - 300 μm in two layers.

3.3.3. Microscopy

Paints rolled on black Leneta sheets were cut with scissors to a size of 10 x 10 mm and deposited on carbon tape. The samples were then observed with a FEI Quanta 250 LVSEM-EDS operating at 12 kV and a pressure of 70 Pa.

Nanometre scale lateral resolution images of surface topography and surface nanomechanical properties were obtained using an atomic force microscope (AFM), Multimode, Nanoscope V, (Bruker®, Santa Barbara, CA), operating in PeakForce® QNM mode. A silicon nitride cantilever, ScanAsyst-Air, (Bruker®, Santa Barbara, CA), was utilised for all experiments. PeakForce® Quantitative NanoMechanics (PeakForce® QNM) is an atomic force microscopy mode that provides high resolution topography imaging and nanomechanical properties such as adhesion and dissipation [83, 84].

In this mode the scanner oscillates in the normal direction with a frequency in the range 0.5 - 4 kHz. While scanning, the AFM feedback loop keeps the chosen applied force constant (Peak Force) by correcting the overall extension of the piezo. A force curve is obtained with every tip contact and its analysis provides the nanomechanical properties which are displayed in the images. The possibility to apply and control very low forces (piconewton range) leads to non-destructive imaging. Drawdowns of the wet paint were made using a 90 µm film applicator on freshly cleaved mica and allowed to dry 24 hours at 23 °C and 50 % relative humidity (r.h.) before observation with AFM.

3.3.4. Profilometry

The surface roughness of the rolled paints were measured using a stylus instrument (DektakXT stylus profiler from Bruker), a contacting technique. A diamond tip with a radius of 2 µm was drawn 10 mm over the surface at a speed of 0.11 mm/s. The distance between each sampling point is 0.37 µm. The force on the tip was set to 0.1 mg. The vertical scan range was set to 524 µm with a vertical resolution of 8 nm in this work.

4. Results

4.1. Thermal stability of commonly used paint components (Paper I)

The results of the XRD analysis on the inorganic pigments are given in Table 11. The sample TiO_2, Kaolin, and Dolomite were identified as pure (> 99%) rutile, kaolinite, and dolomite. The samples Talc and Mica both contained more than one mineral. It is normal that extender pigments contain some impurities as they are produced from natural minerals.

Table 11 Overview of the results from sample evaluation with XRD. Samples marked with * likely to contain some minor impurities other than those presented.

Name of pigment sample	Compound identified by XRD	Chemical Formula
Dolomite	dolomite	$CaMg(CO_3)_2$
Kaolin	kaolinite-1A	$Al_2Si_2O_5(OH)_4$
Talc*	talc clinochlore quartz	$Mg_3Si_4O_{10}(OH)_2$ $(Mg,Al)_6(Si,Al)_4O_{10}(OH)_8$ SiO_2
Mica*	kaolinite muscovite	$Al_2Si_2O_5(OH)_4$ $KAl_2(Si_3Al)O_{10}(OH,F)_2$ or $KAl_2(SiAl)_2O_{10}(OH)_2$
TiO_2	rutile	TiO_2

From the STA data seen in Figure 7a, it was shown that Dolomite was stable at temperatures below 700 °C. The decomposition of the mineral structure occurred through two endothermic reactions at 780 and 880 °C. According to literature, dolomite decomposes in two steps into magnesium oxide and calcium oxide [85, 86] as shown in

$$CaMg(CO_3)_2(s) \rightarrow CaCO_3(s) + MgO(s) + CO_2(g) \quad \text{Eq. 14}$$

$$CaCO_3(s) \rightarrow CaO(s) + CO_2(g) \quad \text{Eq. 15}$$

Theoretically, a sample consisting of pure dolomite would in the first reaction give a mass loss (due to CO_2 emission) of 23.9%, and the second calcination reaction would bring the total mass loss up to 47.7%. The data (Figure 7a) from the experiment showed an acceptable agreement with these theoretical mass losses. XRD analysis of the residues from the STA experiments confirmed that the dolomite had decomposed into MgO (Periclase) and CaO (Lime).

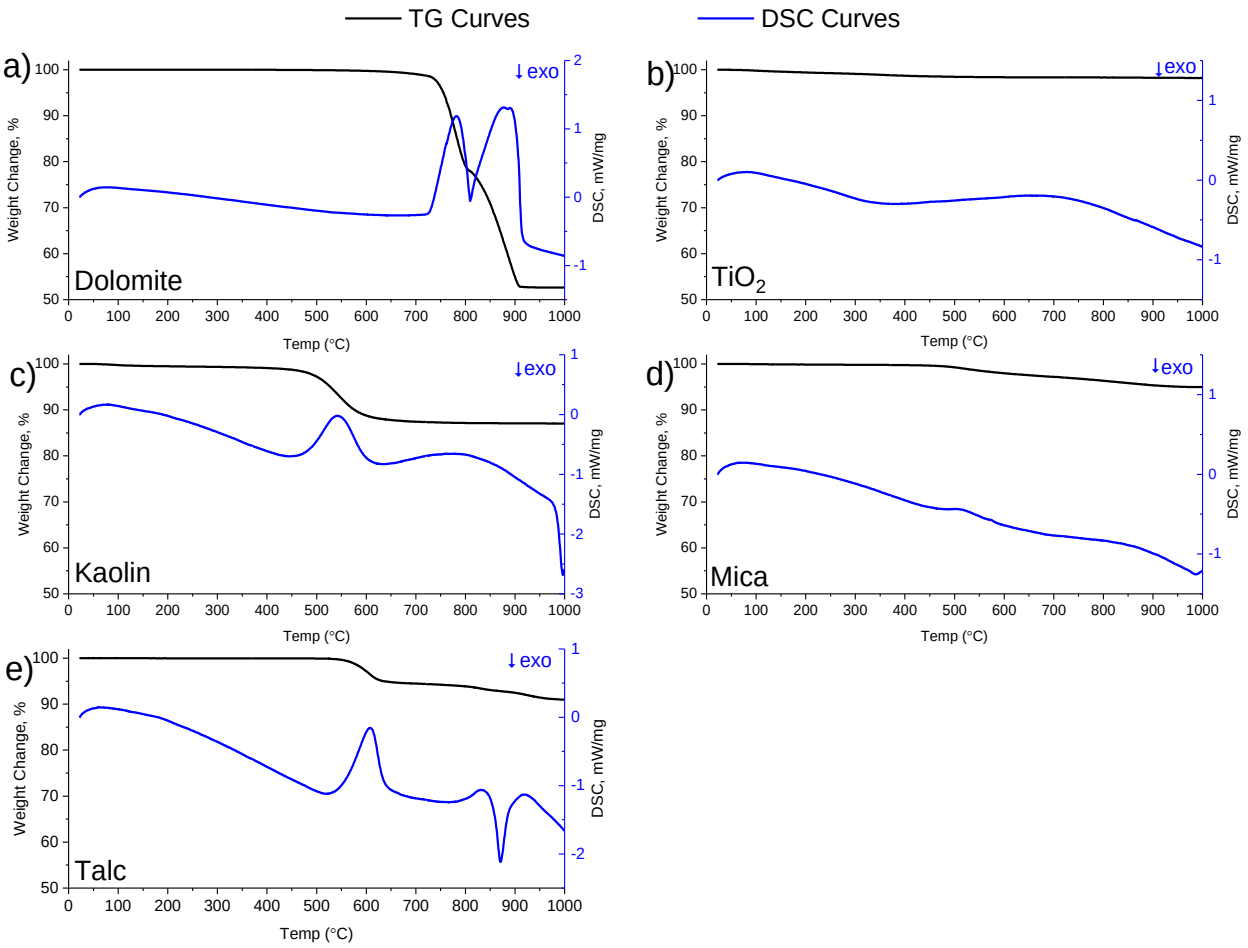

Figure 7 STA thermograms showing TGA curve (black line) and DSC curve (blue line) for a) Dolomite, b) TiO_2, c) Kaolin, d) Mica, and e) Talc. The black line gives weight loss (%) versus temperature (°C). Blue line gives DSC data in which exothermic reactions are given by a negative slope.

According to literature rutile is stable up to temperatures around 1800 °C [87]. XRD analysis, of the sample, TiO_2, before and after the STA experiments where the sample was heated to 1000 °C verified the inert nature of the rutile. However, the data from the TGA, see Figure 7b, showed a total mass loss of roughly 1.5% when the TiO_2 sample was heated up to 1000 °C. Most of the mass loss occurred in the temperature range 100 - 500 °C. Burfield [88] got very similar results when heating a pigment quality TiO_2. It is well known that pigments are commonly treated with compounds to improve their dispersion in the paint systems [89]. Thus, it is probable that the mass loss observed in this work is due to decomposition of such a compound.

The sample Kaolin was identified as the mineral kaolinite by XRD. The STA data shown in Figure 7c detects a small mass loss of around 0.7% in the temperature range of 100 - 500 °C. This could be due to vaporisation of surface water or degradation of a surface coatings. Following this small mass loss, there was a major endothermic reaction that starts at 490 °C and it peaks at 542 °C. Comparing this to literature data [90-92] shows that this was due to the dehydration of kaolin and the formation of meta-kaolin according to

$$Al_2Si_2O_5(OH)_4(s) \rightarrow Al_2Si_2O_7(s) + 2H_2O\,(g) \qquad \text{Eq. 16}$$

The measured mass loss of 13% fits well with the loss of two water molecules per kaolin molecule during the dehydration which would give a mass loss of 14%. At 970 °C a strong exothermic reaction started. This was most likely the transformation of metakaolin into a cubic spinel phase and amorphous silica [90-92] as in

$$2Al_2Si_2O_7(s) \rightarrow Al_4Si_3O_{12}\ (s) + SiO_2(s) \qquad \text{Eq. 17}$$

It is believed that muscovite in the Mica dehydroxylates by the following reaction [93, 94]

$$KAI_2(Si_3Al)O_{10}(OH)_2(s) \rightarrow KAI_2(Si_3Al)O_{11}(s) + H_2O\ (g) \qquad \text{Eq. 18}$$

The dehydroxylation reaction given above gives a theoretical mass loss of 4.5%. This fits well with the final mass loss observed in the TGA experiment, which is showed in Figure 7d. The shape of the TGA curve was similar to the curves found in the literature [93, 94]. At low temperatures, small weight losses were probably due to a loss in surface water. The large wide peak in the range 475 - 950 °C was due to dehydroxylation. The Mica still had a well ordered crystal structure after the TGA experiments. There was not complete agreement of the spectrum prior and after the TGA, so small changes in the crystal structure have probably occurred but this was not investigated further.

The sample named Talc gave an endothermic peak at 607 °C, an endothermic peak at 835 °C followed by an exothermic peak at 870 °C, see Figure 7e. According to a review article made by Wesolowski [95] the first major reaction during heating of talc is an endothermic reaction that dehydrates the material followed by various reactions where different crystalline and amorphous magnesium and silica oxides are formed depending on the temperature. The dehydration of the talc can be described as in [95]

$$Mg_3Si_4O_{10}(OH)_2(s) \rightarrow 3MgO(s) + 4SiO_2(s) + H_2O\ (g) \qquad \text{Eq. 19}$$

where the MgO and the SiO_2 formed are amorphous. The transformation of talc into MgO and SiO_2 would give a theoretical mass loss of 4.8% in the form of water vapour. The total mass loss in the present experiment was closer to 9%. This result, as well as the XRD results described earlier, suggests impurities (see Table 11) in the talc sample. The exothermic peak at 870 °C could be due to the formation of crystalline magnesium and silica oxide compounds but this would not give the large change in mass measured. In addition, no crystalline product could be identified in the XRD-analysis in the residues from the TGA. Therefore they are thought to be amorphous MgO and SiO_2.

By viewing the derivate of weight change with respect to temperature it was seen that binder Sample A, breaks down in two distinct steps in temperatures below 350 °C, see Figure 8. The decomposition continued continuously (no distinct steps due to low experimental resolution) at temperatures over 350 °C to 500 °C until a residue of 5 wt.% of the original sample remained. Binder Sample B, decomposed in a single step in the temperature range of 310 to 400 °C for a non-volatile residue of 3 wt.% of the original sample see Figure 9.

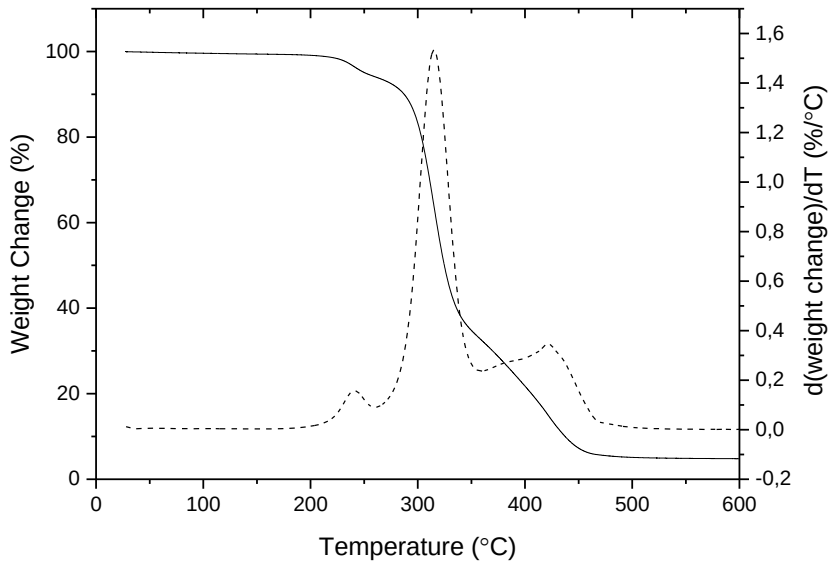

Figure 8 TGA results (weight loss in percent vs. °C) of Pigment A (vinyl acrylic latex) in inert atmosphere. The dashed line is the derivative of weight change in respect to temperature.

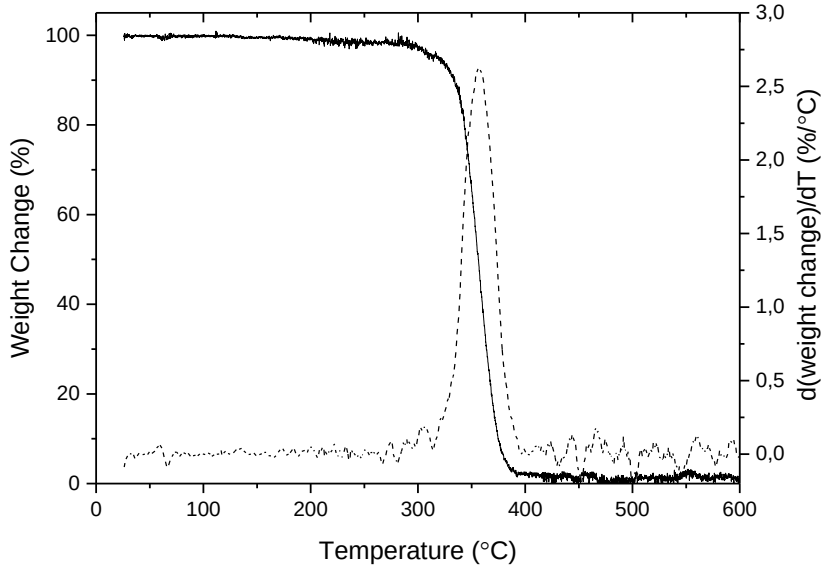

Figure 9 TGA results (weight loss in percent vs. °C) of Pigment B (acrylic latex) in inert atmosphere. The dashed line is the derivative of weight change in respect to temperature.

From the thermogravimetric data presented in Figure 7 - Figure 9, as well as the XRD analysis of the residues, it can be assumed that a pyrolysis process at 500 °C would leave the crystal structure of most of the inorganic pigments used in this study unaffected. Kaolin started to degrade at a temperature just under 500 °C. However, this temperature was high enough to break down the binder samples analysed in this work. Thus, a pyrolysis process operated at temperatures near 500 °C would be able to degrade the organics in a paint and separating them from the inorganic pigments.

However, weight losses were observed of some of the pigments (Kaolin and TiO_2) at rather low temperatures (500 °C and below). These weight changes are most likely due to loss of surface water or due to transformations/breakdowns of the surface coatings of the pigments. As the pyrolysis needs to reach temperatures above 400 °C to decompose the binder, breakdown of the surface coating may be unavoidable in this kind of thermal recovery process. As previously described, surface coatings on the TiO_2 pigment are the major factors affecting their performance in the paint matrix. Thus, even if the crystal core is unaffected by the thermal recycling process, the performance of a recycled pigment may be different to a virgin pigment with intact coating in a paint matrix and may need to be re-coated.

4.1.1. Microwave pyrolysis of liquid (Paint A) and dry (Paint B) paint

The dry content and the inorganic content of the paint samples before pyrolysis experiments, together with the fraction solid residue after the pyrolysis, are presented in Table 12. The fraction of solid residue after the pyrolysis process for Paint A shows a good agreement with the amount of inorganic pigments in the paint. For Paint B the low amount of water in the sample made it difficult to achieve a uniform heating of the material by microwaves, which resulted in incomplete pyrolysis. Large clumps of non-decomposed paint were still present after microwave pyrolysis. In the dry paint (Paint B) the fraction of solid residue after pyrolysis was higher than the initial concentration of inorganic pigments indicating that the solid residue still contained a lot of organic material after the pyrolysis. The two paints, A and B, after pyrolysis are shown in Figure 10. Here the difference is clearly seen where in Paint A the pyrolysis yielded a brittle product coloured black due to the breakdown of the organic component in the paint while Paint B is still white and the large lumps have a foam-like texture due to the incomplete breakdown of the binders. This leads to the conclusion that this type of microwave pyrolysis is not suitable for the treatment of dry paint or non-fluid paint and was not investigated further as a result and due to the fact that it was difficult to control the process parameters.

Table 12 Dry content and amount of inorganic pigments in paint samples in the pyrolysis experiment. Weight fraction of solid residue after the pyrolysis residues after microwave pyrolysis.

Paint sample	A	B
Dry content, prior to pyrolysis	44 wt.%	65 wt.%
Inorganic pigment in formulation	27 wt.%	37 wt.%
Fraction solid residue after the pyrolysis	27 wt.%	64 wt.%

Figure 10 : a) Paint A and b) Paint B after microwave pyrolysis.

4.1.2. The use of microwave pyrolysis recovered pigment in paint formulations

The analysis of the recycled pigment mixture showed that the crystal structure of the two major components, rutile and dolomite, were intact after the pyrolysis-oxidation process. This is consistent with the previously presented results from the TGA experiments. Rutile and dolomite together made up almost 90 wt.% of the total inorganic residue, which made it impossible to draw comprehensive conclusions regarding the heat stability of the other pigments (talc, mica and kaolin) in the recycled paint.

Heat treatment of the solid residue (Figure 11b), in the presence of oxygen (oxidation) significantly increased the whiteness of the sample (Figure 11c). The weight change and the change in colour are due to the oxidation of char carbon to carbon oxides. However, although the whiteness is improved by the heat treatment, it is still far from the whiteness of a mix containing virgin pigments (Figure 11a).

Figure 11: Colour of virgin and recycled pigments where a) mix of virgin pigments corresponding to the one in the pyrolysis ash, b) ground pyrolysis ash from Paint A, c) heat treated (oxidized) pyrolysis ash from Paint A.

The BET specific surface area data for the recovered pigment mixture and the corresponding mixture of virgin pigments are given in Table 13. The specific surface area of the heat-treated residue is significantly smaller (a decrease of 33%) than that of the starting (virgin) pigment mix used in the model paint, showing that an agglomeration of the pigment and extender mixture occurs during the pyrolysis.

Table 13 Result from BET measurements made in triplicates on oxidized recovered pigment mixture from the pyrolysis process and a mix of corresponding virgin pigments.

Sample	BET (m^2/g)	
	Average	Std. Dev
Recovered pigment mixture	6.53	0.37
Pigment mix	9.71	0.31

The recycled pigment material was not fully dispersed into the paint system, resulting in the film defects (lumps) seen in the lower half of Figure 12. This effect was seen even when increased dispersant levels were added to the formulation. From the specific surface area and the lower portion of the photo, it is clear that some agglomeration of the mineral particles occurs during the microwave pyrolysis-oxidation process.

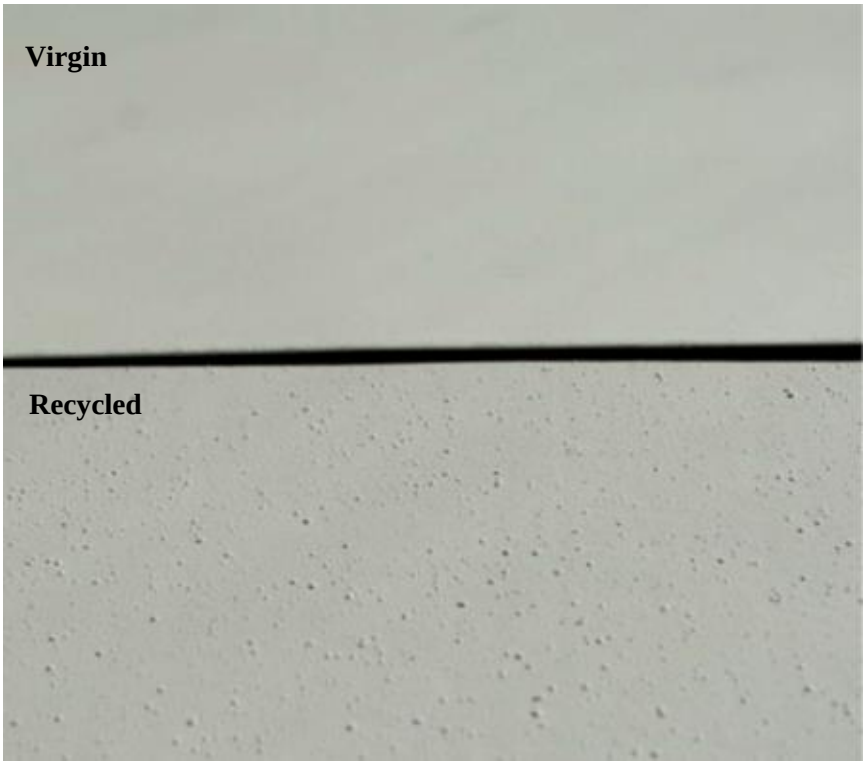

Figure 12 Photo of paint films made with virgin pigments (upper panel) and recycled pigments (lower panel). Dry film thickness of both paint films are 100 µm. The actual length of the paint sample shown is 10 cm.

The surface painted with the test paint containing recycled components was also studied using SEM-EDX in order to investigate what had caused the formation of lumps. A typical result is shown in Figure 13. Only the EDX map for Ti is shown but maps for other elements were recorded and evaluated as well. The SEM-EDX results showed that agglomeration of particles with high Ti content, i.e. rutile particles, while all other analysed elements (Al, Ca, Si, Mg) were well dispersed in the paint film.

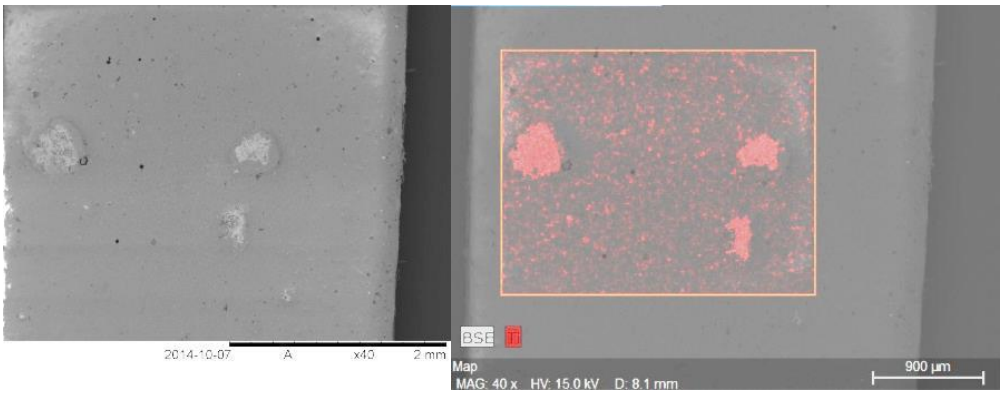

Figure 13 SEM micrograph of the recycled paint surface (left) and EDX element map for Ti (right).

It is possible that the TiO_2-rich lumps have been formed in the paint due to inferior dispersion. Destruction of the surface coating on the TiO_2 particles could be the cause of this. The nature of the surface coating applied to the specific rutile pigment used here was not stated in the data provided by the manufacturer. Both inorganic coatings, based on alumina or silica, and organic coatings are commonly used in the pigment industry [14]. Since the pigment rutile used in this work showed a weight loss during the thermo-gravimetric experiments, it is highly probable that it had an organic coating and that this coating was destroyed during pyrolysis.

The measured paint qualities of the two paint formulations made with recycled pigments and virgin pigments are summarized in Table 14. The opacity of the paints based on recycled material is higher than those of the paints based on virgin material. This outcome is a false positive result as the lower whiteness of the recycled material influences the spreading rate calculations (this method includes absorption and scatter contributions, so the colour will have an impact on the observations). There was a slight decrease of durability in paints based on recycled material (probably caused by the increased dispersant levels) while the gloss was equivalent for each pigment (the film defect problem is hidden by matt formulations).

Table 14 Paint parameters for paint based on virgin and recycled material.

	Method	**High PVC formulation 1 with virgin material**	**High PVC formulation 1 with pyrolysis ash**	**High PVC formulation 2 with virgin material**	**High PVC formulation 2 with pyrolysis ash**
Opacity (98 Spreading Rate)	ISO 6504-3 [96]	8.3	11.0	5.6	7.6
Whiteness	ASTM E313 [97]	83.15	78.11	80.90	74.75
Yellowness	ASTM E313 [97]	2.88	3.34	3.50	3.80
Gloss (85º)	ISO 2813 [98]	14.9	12.3	10.4	9.6
Durability (scrub resistance)	ISO 11998 [99]	0.9	1.3	8.9	11.1
Colour difference	ISO 11664-6 [82]	N/A	1.1	N/A	1.6

From these experimental results, it can be concluded that recycled pigments treated as described above cannot be used as a direct replacement in paint formulations. However, before the material can be approved or rejected for use in paint formulating the issues of poor dispersion and colour change needed to be resolved. Which lead to the investigation of the TiO_2 pigments specifically as described in the following sections.

4.2. Surface properties of recovered TiO_2 from paint waste (Paper II/III)

The average weight of the solid residue after the pyrolysis step was 32.5 ± 0.04, 32.8 ± 0.3 and 32.8 ± 0.2 wt.% of the original paints for Pigment A, Pigment B, and Pigment C respectively. After the oxidation step, 30.4 ± 0.1 wt.% of the original paint mass remained for Pigment A and B, while 30.5 ± 0.2 wt.% was left after oxidation of paint containing Pigment C. These values are in good agreement with the 30.47 wt.% pigment that was in the processed paint formulation as shown in Table 9. There was no visible difference in colour between the virgin pigments and the recycled pigments after oxidation, which indicates that it is possible to extract TiO_2 from the paint matrix by means of pyrolysis and oxidation.

The results from measurements of conductivity and ion concentration in the 10 wt.% pigment suspensions are listed in Table 15. Measured ions not listed can be assumed to have a concentration < 1 mM. A general trend could be found here; ion concentration and *de facto* conductivity were higher for recovered pigments compared to virgin pigments before washing. The increase in ion concentration could have a negative effect on the stability of the dispersion [25] and the functionality of used dispersants in a paint system [75] so it was of importance to remove the excess ions from the solution.

Table 15 Conductivity and selected ion concentration of 10 wt.% pigment suspensions given in mM. Samples measured after 96 h stirring. Unless otherwise stated the uncertainty of measurement is 10%.

Sample Description	Conductivity [mS/cm]	Na [mM]	Al [mM]	Si [mM]	Ti [mM]	P [mM]	Cl [mM]
Virgin Pigment A	0.1 ± 0.1	1	< 0.1	< 0.1	< 0.1	< 0.1	-
Virgin Pigment B	0.1 ± 0.1	1	< 0.1	< 0.1	< 0.1	< 0.1	-
Virgin Pigment C	0.2 ± 0.1	11	< 0.1	< 0.1	< 0.1	< 0.1	0.2 ± 0.1
Oxidized Pigment A[1]	1.00 ± 0.1	20	3	0.3	0.6	1	-
Oxidized Pigment B[1]	0.6 ± 0.1	10	0.2	0.1	0.1	< 0.1	-
Oxidized Pigment C[1]	2.4 ± 0.1	130	13± 2	< 0.1	< 0.1	< 0.1	0.1 ± 0.1
Recycled Pigment A[2]	< 0.01	< 1.0	< 0.1	< 0.1	< 0.1	< 0.1	-
Recycled Pigment B[2]	< 0.01	< 1.0	< 0.1	< 0.1	< 0.1	< 0.1	-
Recycled Pigment C[2]	< 0.01	< 0.1	< 0.1	< 0.1	< 0.1	< 0.1	

[1] pigments after pyrolysis and oxidation
[2] pigments after pyrolysis, oxidation, and washing
- not measured

The increase in Na and P concentration in the oxidized pigments most likely comes from the degraded surface active compounds normally used in coating formulations [33]. Surface active compounds such as phosphate esters are used to create stable suspensions of both pigments and of latex particles. These elements can always be expected to be found within a recycled pigment. It is most probable that Ti, Al, and Si came from the dissolution of the pigment particle itself. Ti comes from the rutile core of the pigment, while Al and Si come from the coating surrounding/encapsulating the particle surface.

The XRD analysis of the residue confirmed that the rutile structure of the recycled pigments was intact. This was as expected, because the temperatures in the recovery process are relatively low and the results are analogous with the results in Section 4.1.

4.2.1. XPS data

4.2.1.1. Pigment A

For both the virgin and the recycled samples, C, Ti, Al, and O were clearly detected along with small amounts (< 1 atomic %) of P and Zr. The peaks for Ti 3p/2 and Ti p1/2 were located at 458.3 and 464.1 eV respectively as shown in Figure 14a. Both peaks were identical, at the same position, and corresponded well with published data for TiO_2 [100].

Figure 14b shows the spectrum for Al 2p. The centre of this peak for the recycled material shifted from 74.1 eV to 74.4 eV and displayed a shoulder at higher energies when compared to the peak for the virgin material. Due to the small differences in the position of Al 2p for different alumina (hydr)oxides [101] the position of O 1s is normally used as a complement to the Al 2p position [102] for identification of compounds. As the samples had different surface coatings, complete identification was complex. Nonetheless, it has previously been shown that the partial dehydration of surface aluminium hydroxide may shift the shape of the Al 2p to that of aluminium oxide (Υ- Al_2O_3) [103], which is similar to the shift observed between the virgin and the recycled pigment in this work. A larger fraction of the O 1s curve seen in Figure 14c was shifted from 531.7 eV to 529.8 eV. This also indicated a less hydroxylated surface and more contribution from the O^{2-} in the bulk phase of the oxide [102].

The concentration of P being relatively small made it difficult to make an accurate determination of its chemical state/composition. However, as the P 2p peaks (Figure 14d) for the virgin and the recycled pigment were centred on the same energy, 133.9 eV, it can be suggested that there was no change in chemical state due to the recycling process, and it could possibly be a phosphite or dihydrogen phosphate compound [104]. It has previously been shown [105] that the P-O bond should be intact in temperatures used in the recycling process.

The Zr $3d_{5/2}$ and Zr $3d_{3/2}$ peaks were located at 182.5 eV and 184.8 eV respectively for both the virgin and the recycled pigment (see Figure 14e.). Zirconium was present in low concentrations, however, it was most likely zirconium oxide [106, 107] which also appeared to be unaffected by the recycling process.

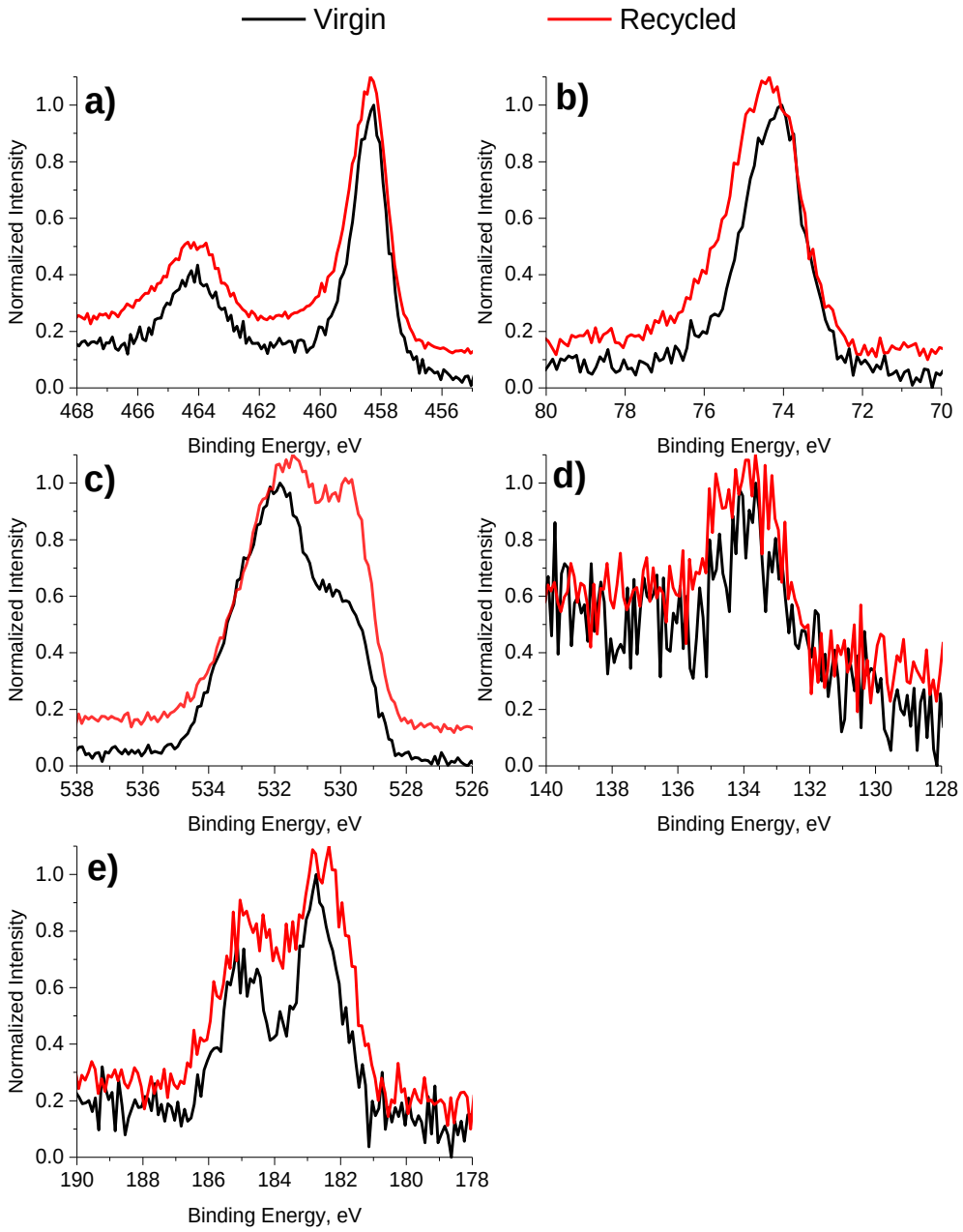

Figure 14 XPS photoelectron peaks a) Ti 2p, b) Al 2p, c) O 1s d) P 2p and e) Zr 3d for virgin (black line) and recycled Pigment A (red line). The intensity is normalised, peaks are relative to binding energy of adventitious C 1s = 284.8 eV. The recycled pigment spectra is offset 0.1 units in intensity for readability.

Another aspect of importance is the concentration of the different species. This is especially important for the performance of the pigment. One of the most important characteristics for a coated pigment is the ratio of bulk Ti to coating elements [108-110]. The depth profiles of the atomic-ratio of Al to Ti for the virgin and recycled pigments are shown in Figure 15. The depth profile of the recycled pigment showed a minor decrease in the Al concentration at the surface. The increased Al concentration in the suspension of the recycled Pigment A (Table 15) also suggested that the Al coating was partially degraded by the heat treatment.

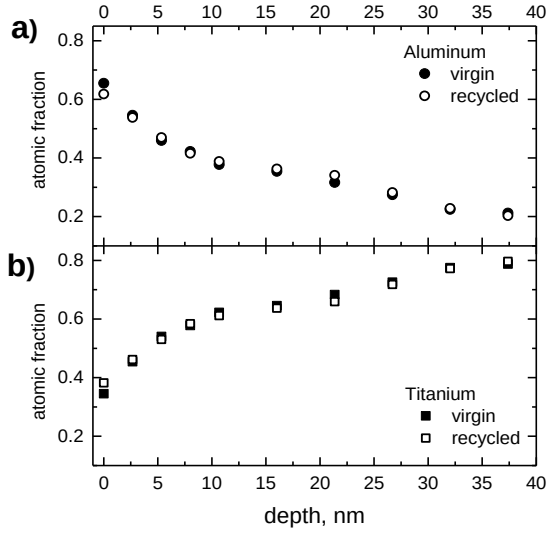

Figure 15 XPS cation depth profile of a) aluminium and b) titanium. Closed symbols are for virgin and open symbols are for recycled Pigment A.

4.2.1.2. Pigment B

For both the virgin and the recycled pigments, peaks for C, O, Ti, Al and Si were identified. There were no significant shifts in peak position or widening of peaks before or after the recycling process as shown in Figure 16a - d, indicating that the chemical state of all the components remained unaltered after the recycling process. The Ti $2p_{3/2}$ and Ti $2p_{1/2}$ peaks were (Figure 16a) located at 458.7 eV and 464.5 eV respectively. Similar to Pigment A, this also corresponded well with TiO_2 [100]. However the slightly higher binding energy compared to Pigment A suggests that this quality has a slightly higher concentration of Ti^{4+} than Ti^{3+} at the surface.

The Si 2p peaks for both pigments were centred at 102.7 eV (Figure 16b). Normally, pure SiO_2, is proposed as one of the components in coatings for pigment [3]. However, the Si 2p peak for pure SiO_2 has been reported to be located at higher binding energies (around 103.5 eV) [111]. It was more likely that the Si on the pigment particles was incorporated in a Si-Al-oxide kaolinite-like structure [112]. O 1s at 532.1 eV (Figure 16c) and Al 2p at 74.5 eV (Figure 16d) further supported the conclusion that the Si and Al were combined as an alumina silicate mixture [112]. Morris et. al. [21] also studied rutile coated with Al and Si and found that the coating consisted of an octahedral alumino-silicate mixture. Furthermore, with TEM imaging, it was concluded by these researchers that the silica was deposited as a thin layer covering the rutile core, while the alumina formed a rough sheet-like coating on top. This is an important observation as an aluminium-silicate is not as thermally stable [113] as pure SiO_2 structures [90].

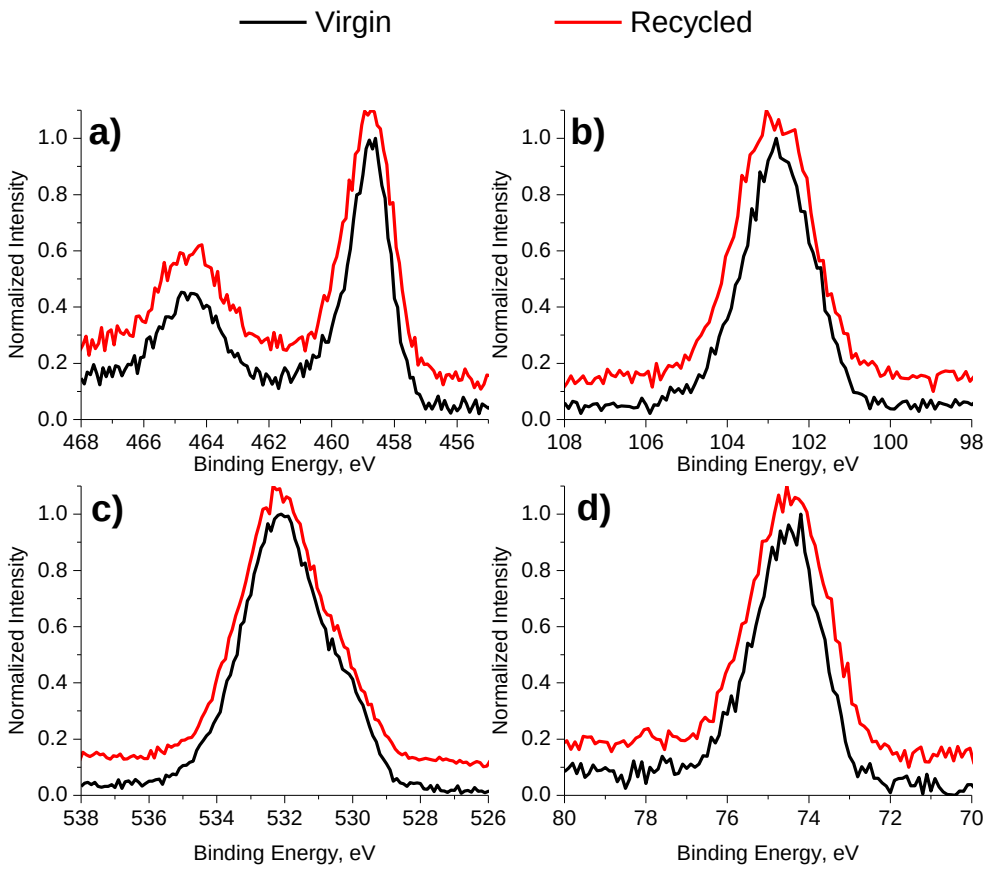

Figure 16 XPS photoelectron peaks of a) Ti 2p, b) Si 2p, c) O 1s and d) Al 2p for virgin (black line) and recycled Pigment B (red line). The intensity is normalised and binding energies are relative to C 1s = 284.8 eV. The recycled pigment spectra is offset 0.1 units for readability.

As previously mentioned, the chemical state of all the surface species remained almost intact, but the atomic ratio of the species did not. Figure 17 shows the cation depth profile of Al, Si and Ti for virgin and recycled Pigment B. After the recycling process, the relative amount of Al had been reduced while Si concentration was increased at the surface. This implies that part of the outermost layer of alumina oxide had been etched away, exposing the silica oxide layer underneath.

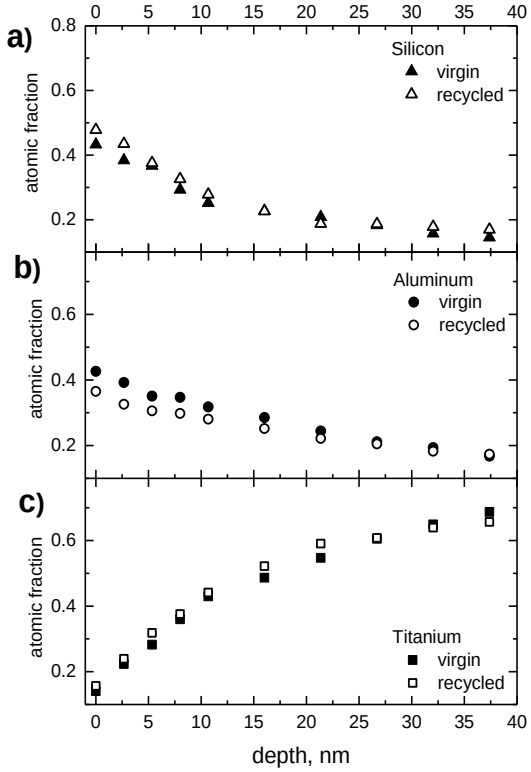

Figure 17 XPS cation depth profile of a) silicon, b) aluminium, and c) titanium. Closed symbols are for virgin and open symbols are for recycled Pigment B.

4.2.1.3. Pigment C

In the XPS spectrum for Pigment C, five elements were distinctly detected: C, Ti, Al, Si, and O. The peaks for Ti $p_{3/2}$ and Ti $p_{1/2}$ (shown in Figure 18a) were located at 458.2 and 463.8 eV respectively, as expected for TiO_2 [114]. In Figure 18d it can be seen that the Al 2p peak is located at 74.1 eV for both samples. This matches the binding energy of an alumina oxide, i.e. Al_2O_3, Al(OOH) or $Al(OH)_3$. No further investigation was carried out to investigate the exact nature of the aluminium species, as this task is complex [102] and outside the scope of this study.

The centre of the Si 2p peak for both the virgin and the recycled was located on 102.1 eV (Figure 18b). It is common to coat pigments with silica (crystalline or amorphous SiO_2), but the Si 2p peak at 102.1 eV did not correspond to the binding energy of SiO_2, which is located at higher energies (around 103.5 eV) [111]. This suggests that the silicon is in the valence state +3 [111]. Compared to Pigment B the Si was only present on the immediate surface (< 5 nm in depth) and the positions of Si 2p and Al 2p peaks did not fit with an alumina silicate mixture [112], thus indicating that Si was a contaminant that has accumulated at the surface.

It should also be mentioned that siloxane compounds provided a good fit of the peaks, with Si 2p, O 1s and C 1s at 102.1, 532.4 and 284.4 eV respectively [115]. These types of compounds are sometimes used to improve the dry flow of pigment particles [3]. On the other hand they also make the particles more hydrophobic and thus less useful in most coating applications [3]. It has also been reported that these kind of compounds degrade in the temperature range [116] used in the recovery process presented in this thesis. As the Si 2p is clearly visible in both the virgin and the recycled sample, it is more likely that the Si is incorporated in the matrix as a contaminant rather than in the form of a siloxane compound.

In comparison with the other element peaks, the O 1s signal showed more pronounced differences between the virgin and the recycled pigment (Figure 18c). Whereas the main centre of the peaks was at the same binding energy, the virgin sample exhibited a shoulder towards lower energies while the recycled sample has a shoulder towards higher energies. The explanation of this difference is not obvious and cannot reasonably be attributed to an alteration of the surface species, as all the other major elements exhibited minor changes. It has previously been documented that three different O 1s peaks can be observed for metal oxides [117, 118]. The lowest energy peak (around 529 eV) is from the contribution of the O^{2-} oxygen atoms belonging to the oxide bulk structure. The second peak, around 532 eV, is due to surface hydroxyl groups. The third peak, with the highest energy at roughly 534 eV, is from chemisorbed water. As the other components have their chemical state intact, the most likely explanation is a difference in the concentration of water that has been chemisorbed from the ambient surroundings on to the surfaces. This chemisorbed water would increase intensity at higher energies. It is also possible that the water could cover the surface and reduce the measured intensity at lower energies (bulk O^{2-} oxygen). The alteration in the O 1s spectrum is probably not coming from an actual chemical change but rather from an increased amount of chemisorbed water on the recycled pigment compared to the virgin pigment.

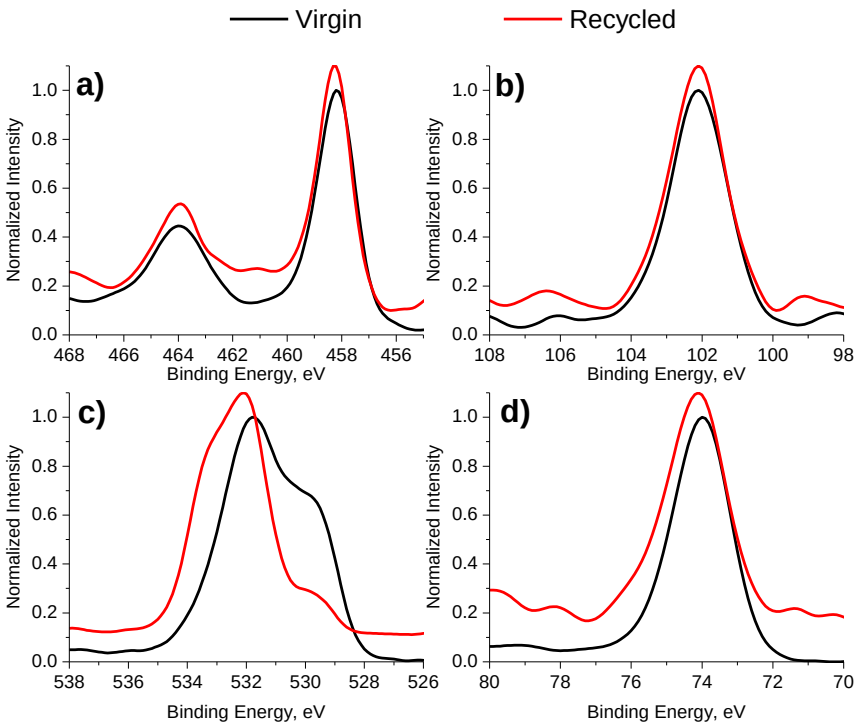

Figure 18 XPS photoelectron peaks of a) Ti 2p, b) Si 2p, c) O 1s and d) Al 2p for virgin (black line) and recycled Pigment C red line). The intensity is normalised and binding energies are relative to C 1s = 284.8 eV. The recycled pigment spectra is offset 0.1 units for readability.

In Figure 19, a depth profile for the ratio between Ti and Al is shown for the virgin pigment and the recycled pigment. Si was excluded as its chemical state does not suggest a traditional coating characteristic. As seen in Figure 19, the ratio of Ti and Al is intact at the surface after recycling. However, going further into the particles the Al seems to drop in concentration more rapidly than for the virgin pigment. This indicates that some of the coating has been etched away during the recycling process. This corresponds well with the increased Al concentration measured in a suspension of non-purified recycled pigments (see Table 15). Overall, it seems that the recycling process does not alter the surface by the creation of new species but it slightly reduces the thickness of the alumina coating.

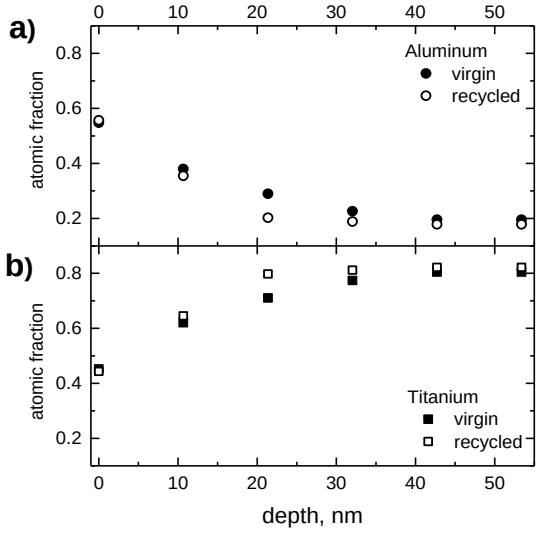

Figure 19 XPS cation depth profile of a) aluminium and b) titanium. Closed symbols are for virgin and open symbols are for recycled Pigment C.

4.2.2. Particle size and specific surface area

The optimum particle size for TiO_2 pigments to scatter visible light is about 0.2 - 0.3 μm [46]. As can be seen from Figure 20, the recycling process does not have any significant effect on particle size distribution for either pigment. Minor differences could be noted in the distribution of the particle size and the recycled samples had a slightly broader distribution. However, this difference is minor so the overall effect on a final pigmented coating can assumed to be insignificant.

Published specific surface areas for rutile pigments with various coatings lie in the range of 5 to 35 m^2/g with the majority around 20 m^2/g [21, 108, 109, 119, 120]. The specific surface area for virgin Pigment A, B and C was shown to be 18, 11 and 17 m^2/g respectively. After the recycling process, the specific surface area for Pigment A, B and C was 16, 11 and 16 m^2/g respectively. The decrease in surface area can be due to increased particle size (the particles were not treated with ultrasound before BET measurement) or a decrease in the number of surface hydroxyl groups after the thermal treatment [121].

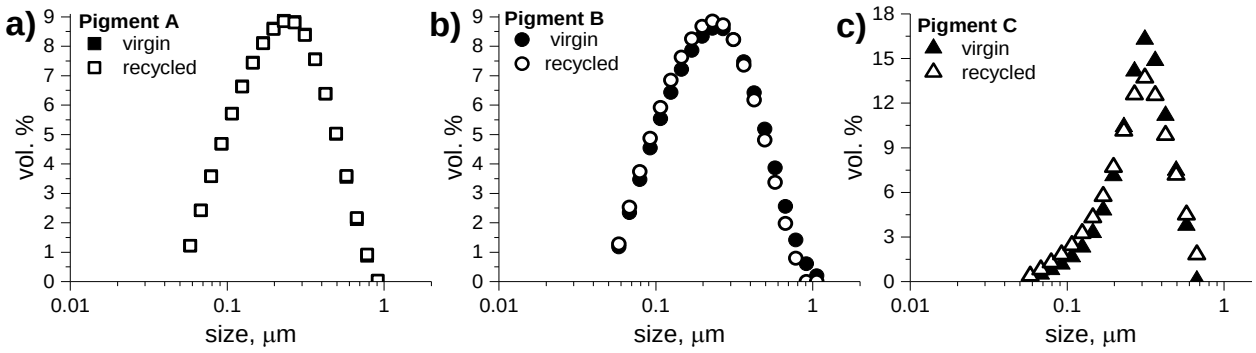

Figure 20 Particle size distribution expressed as volume percent for a) Pigment A, b) Pigment B, c) Pigment C. Data points for virgin materials are solid and data points for recycled materials are open.

4.2.3. Dynamic mobility and zeta potential

The measured zeta potential is shown in Figure 21 for virgin and recycled Pigment A (a - c), Pigment B (d - f), and Pigment C (g - i). The corresponding isoelectric points (IEPs) are given in Table 16. The IEP of a mixed oxide tends to be the surface average of its components [122]. This has previously been shown to be the case for rutile pigments coated with Al and Si [21]. Reference IEP values for coated rutile pigments are given in Table 17, with most pigment qualities having an IEP in the pH range of 7 - 8.

The first noticeable difference between recycled and virgin pigment was the reduction in magnitude of the zeta potential over most of the pH range. Commonly, decorative waterborne paint has a pH range of 7 - 9 so this is the most important region. While for Pigment A, the recycling step induced only minor changes (around 5mV of loss at pH 7-9) for Pigment B, the difference in zeta potential between the virgin and recycled pigments was over 10mV in the same pH region. This was significantly reflected by the changes noted for the IEP and was noticed regardless of the salt used as background electrolyte and of its concentration.

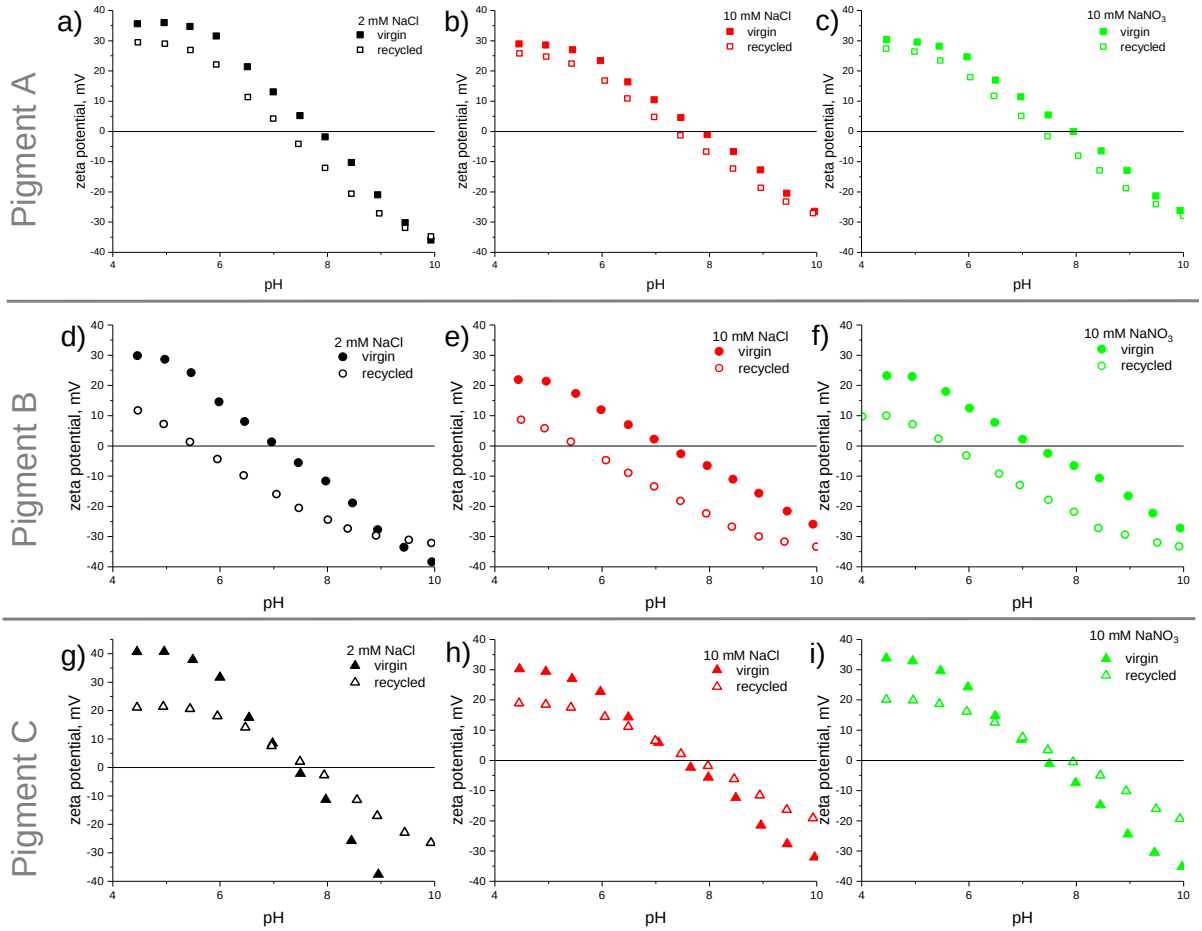

Figure 21 Zeta potential as function of pH for 5 wt.% suspensions of virgin and recycled pigments.

Table 16 Experimentally determined IEPs for virgin and recycled pigments measured in 5 wt.% suspensions.

Sample	Electrolyte	Virgin IEP	Recycled IEP
Pigment A	2 mM NaCl	7.8	7.2
	10 mM NaCl	7.8	7.3
	10 mM $NaNO_3$	7.9	7.3
Pigment B	2 mM NaCl	7.0	5.6
	10 mM NaCl	7.1	5.5
	10 mM $NaNO_3$	7.2	5.7
Pigment C	2 mM NaCl	7.4	7.6
	10 mM NaCl	7.4	7.6
	10 mM $NaNO_3$	7.4	7.8

Table 17 IEP values for commonly used coated TiO_2 pigments.

Pigment	IEP	Source
Pigments coated with alumina and zirconia	7.8 ± 0.3	[120]
Pigment coated with alumina and silica	2.8 - 8.1	[108, 109]
Pigment coated with alumina	8.2 - 9.2	[110]

According to the XPS data, the surface of Pigment A consists of a combination of TiO_2 and an Al (hydr)oxide. Different IEPs for these oxides have been reported in literature [45] but the consensus is that TiO_2 has an acidic IEP (around pH 5 - 6) and Al (hydr)oxides have an IEP in the alkaline area (≥ pH 9). The XPS depth profile in Figure 15 showed a small decrease in the ratio of Al to Ti on the surface of the recycled pigment compared to the virgin pigment. This decrease in Al would lower the overall IEP of the recycled pigment as observed in Figure 21.

Recycled Pigment B showed a larger decrease in IEP compared to Pigment A. It is known that silicon oxides are more acidic (IEP < pH 3) [45] than TiO_2 and aluminium oxides. The XPS data for Pigment B (Figure 17) showed a large decrease in the Al to Si ratio at the surface after the recycling process, which is most likely due to etching away of the Al layer, exposing the Si layer. This could explain the displacement of the IEP to more acidic pH due to the recycling process.

Pigment C showed a slightly different behaviour compared to the other two pigments. The ratio of the Al to Ti on the surface was, according to the XPS measured, unaffected by the recycled process and the IEP was almost the unaltered. However, the magnitude in zeta potential for the recycled pigment was around 10 mV lower compared to the virgin pigment in pH 7 - 9. It has previously been shown [123] that temperatures used in the recycling process can reduce the concentration of hydroxyl groups on surfaces. A lower concentration of hydroxyl groups would result in a lower magnitude in zeta potentials, as fewer groups are available for protonation/deprotonation. For electrostatically stabilized systems it is generally agreed that a large magnitude of the zeta potential variation usually results in more stable particle suspension. In practice, the lower magnitude observed may come from partial dehydroxylation, which implies that the dispersibility by the surface active agent would be less effective.

The correlation between the nature of the coating and the final IEP of TiO_2 pigments has been shown previously [21] to influence the rheology [21, 124, 125] and the stability [125] of a pigment suspension, and the performance of pigment dispersants that are commonly used in coating formulations [124]. The importance of the alumina coating has been shown particularly when dispersing TiO_2 pigments with anionic surfactants in slightly alkaline conditions [124]. [124]. In that sense, Pigment A and Pigment C can be regarded more potentially more suitable for further reuse than Pigment B.

The change in IEP for Pigment A due to the recycling process was roughly 0.5 pH-units and even less for Pigment C (see Table 16) when compared to the corresponding virgin pigment. This variation can be regarded as negligible as the three virgin pigments have a larger difference than this. However, multiple recycling loops could potentially cause further degradation of the coating, leading to larger difference and impacting the pigment usability. The recycled Pigment B had an IEP difference that was substantially larger, approximately 1.5 pH-units lower than that of the virgin pigment. In practical application, this difference implies major formulation changes which would render the particle use more limited. Pigment A showed a slightly more acidic surface due to degradation of the alumina coating, while Pigment B showed a vastly more acidic surface after the recycling due to the increased presence of Si-species. This confirms that the nature of the coating on the pigment is important and the recycling process proposed in this work will affect different rutile pigments differently.

4.2.4. Summary - surface properties of recovered TiO_2

XRD showed that the rutile cores of all pigments were intact after the recycling process. In addition, it was shown that there were no major changes in the particle size distribution or surface area for each pigment during the recycling process.

XPS results indicated that there were no major changes in the chemical state of the surface species in either pigment after the recycling process. The recycling process seems to cause partial dehydration of the aluminium hydroxide coating of Pigment A. However, this is probably not a major problem as alumina hydroxide is known to reform through rehydration of aluminium oxide over time [126]. The breakdown of the coating, as seen for recycled Pigment B, is a source of concern, however. The depth profile of Al for recycled Pigment A and Pigment C showed minor degradation while recycled Pigment B showed a major change in the atomic ratios between Si, Al and Ti after the recycling process. This shows that Pigment B was less resistant to the recycling process than Pigment A and Pigment C.

Results from the zeta potential measurements also support XPS data where Pigment A and Pigment C showed minor coating degradation while for Pigment B this was more severe. Therefore it can be concluded that differently coated pigments are more or less susceptible to degradation by the thermal recycling process.

4.3. Characterization of paint formulated using recovered TiO_2 (Paper IV)

Virgin and recycled Pigment C was used in a paint formulation as described in Section 3.3. The results of the measurements on the paints based on virgin and recycled pigment and on the painted surfaces are presented here. In general the results of the absolute measurement values are of minor interest while the relative difference between the two paint samples is of major importance.

Both paints (using recycled and virgin Pigment C) yielded the same measured pH-value of 9.1 ± 0.1. This falls within the range of what was expected for an emulsion paint. Using the recycled pigment did not show any impact on the pH of the paint.

The results from the viscosity measurements are shown in Table 18. There was a slight variation in the ICI viscosity but the differences were too small to have a relevant impact on the paint. The difference in Stormer viscosity between the samples before storage, 110 KU for virgin and 104 KU for recycled pigment, is not substantial but may be noticeable for a professional painter. However, the difference in Stormer viscosity may be corrected by adjusting the thickener concentration in the paint formulation. Both samples show a slight decrease in Stormer viscosity after storage. It is not unusual to get slight changes in viscosity after stability testing. Major changes in viscosity, syneresis, or gel formation would be a reason for concern, but none were observed for the paint samples presented here.

Table 18 Viscosity values of paint samples based on virgin and recycled Pigment C, respectively. Samples were measured 24 h after fabrication and after stability test (5 weeks in 50 °C).

Sample	24 h after fabrication		After stability test	
	Virgin pigment	Recycled pigment	Virgin pigment	Recycled pigment
Stormer [KU]	110	104	106	102
ICI [P]	0.59	0.65	0.63	0.70

The colour coordinates for the two paint films are presented in Table 19. The colour difference between the two films is summed up to ΔE2000 = 0.51. This difference is on the limit of what the human eye can detect [80], and for many practical applications this difference is acceptable.

Table 19 L*, a*, and b* values for paints based on virgin and recycled pigments.

	Virgin pigment	Recycled pigment
L*	97.28	96.85
a*	-0.82	-0.63
b*	1.08	1.42
ΔE2000	Reference	0.51

The recycled pigment gave a slight decrease in hiding power compared to the virgin pigment as shown in Table 20. This, combined with the significant decrease in gloss (Table 20), suggests that the recycled TiO_2 was aggregated, thus not having the right particle size distribution for optimum light scattering.

Table 20 Hiding power measured in the form of contrast ratio Y_w/Y_b of paints based on virgin and recycled Pigment C where Y_w and Y_b represent the measurement value on white and black backgrounds respectively. Gloss measured in angles 20°, 60°, and 85° to the paint film.

	Virgin pigment	Recycled pigment
Contrast ratio	98.1%	97.3%
Gloss 20°	32.4	5.3
Gloss 60°	73.5	22.0
Gloss 85°	92.0	17.3

The particle size measurements that were made previously (Figure 20) did not suggest that the recycled pigment was more aggregated than its virgin counterpart. However, before these measurements were made, ultrasound was applied to the suspension, and the measurements were taken on a small sample size (< 0.1 wt.% of the total amount used to produce the paint). Surface characterization of the pigments Section 4.2 did not indicate any major differences in surface chemistry between the pigments. Furthermore, the properties of the paints after the stability test (Table 18) do not suggest that there was a problem with the colloidal stability of either paint.

Therefore, the most likely reason for aggregates in the paint based on recycled pigment is that the pigments were aggregated during the recycling process. The shear forces in the milling of the paint during manufacturing were not sufficient to de-agglomerate the recycled pigment.

SEM micrographs for paint films using virgin and recycled TiO_2 Pigment C are shown in Figure 22. A comparison of the micrographs revealed a substantial difference between the paint based on the virgin pigment and the paint containing the recycled pigment. Paint films using the virgin pigment are rather smooth, whereas, Figure 22b confirmed the formation of aggregates in the paint made with recycled pigment with the largest aggregates being approximately 100 µm in diameter. No significant difference between the paints regarding the atomic composition or spatial distribution of the atoms was observed from the EDS data. The overall composition of the paint did not change, however, the performance of the paint regarding such properties as gloss decreases due to agglomeration.

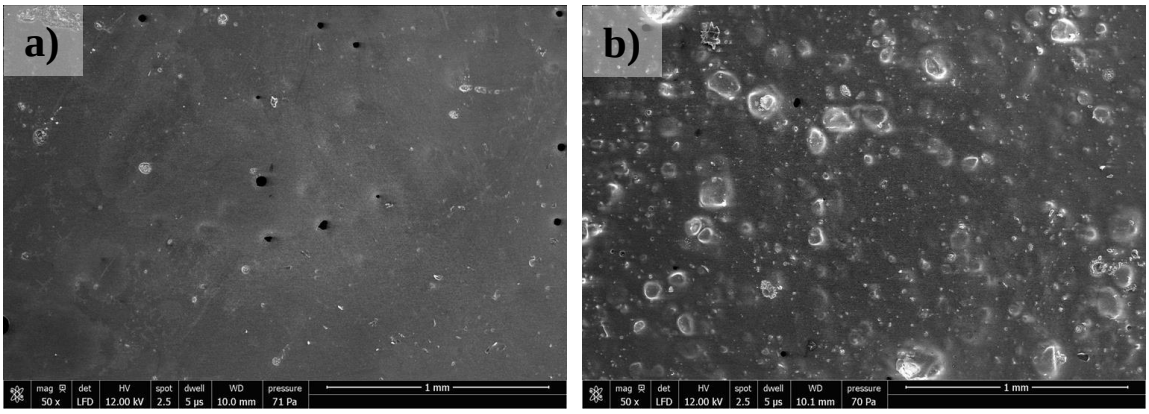

Figure 22 Micrographs of paint using a) virgin Pigment C and b) recycled Pigment C. 50x magnification.

The microstructure and adhesion were investigated by AFM on the paint film surface for virgin and recycled based paints as shown in Figure 23. Compared to profilometry, AFM looks at smaller scales and could focus on the details of the films. From the height images (top and bottom, left), little difference could be observed, except for maybe a slightly rougher character in the case of the films based on recycled pigment. The topographic images are slightly blurred, this is most likely due to the thin layer of surfactant covering the surface of the paint films as suggested by the adhesion micrograph. Below the surfactant is the more adhesive latex film (data not shown). This was expected considering the paint formulations were the same except that the pigment was changed.

Interestingly, no difference could be seen for the adhesion pictures (top and bottom, right). The hills correspond to low adhesion (dark areas) in the adhesion images. These areas are likely to be the TiO_2 pigment which appears (on this length scale) to be well distributed throughout the paint films.

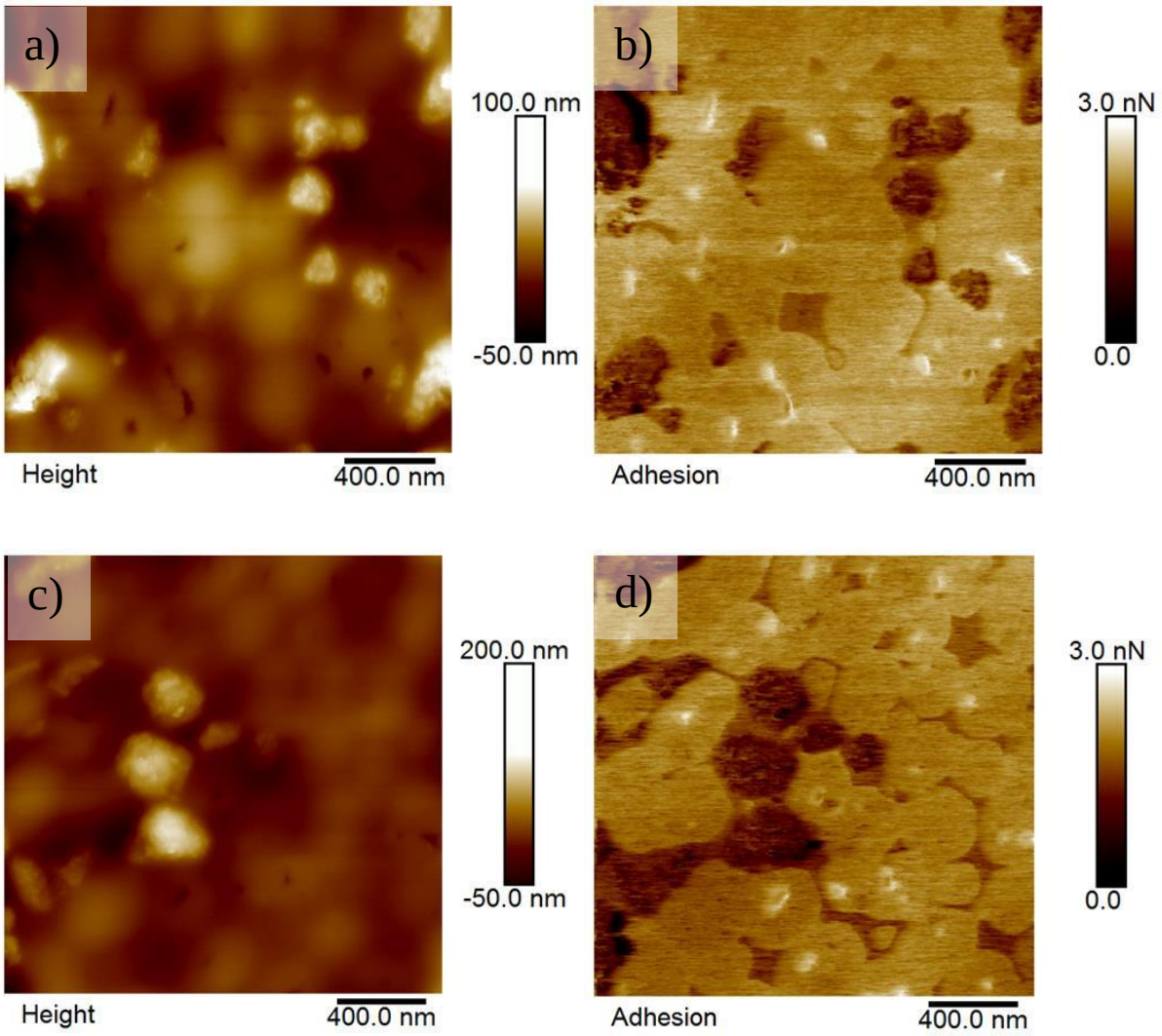

Figure 23 AFM of paint film based on virgin and recycled pigment. a) is topography and b) is adhesion for virgin pigment. c) is topography and d) is adhesion for recycled pigment. Light is up and dark is down in the topographic image, and light is high adhesion while dark is low adhesion in the adhesion image.

The surface structure and roughness of the hand-rolled virgin and recycled pigment based paint films are shown in Figure 24a-b. Compared to AFM, profilometry looks at a larger scale, more relevant for the visual appearance of the films. For both paint films shown in Figure 24a-b the surface structure was fairly rough with hills and valleys up to 100 µm apart. Both types of paint show a long waviness profile which comes from the application method of using a hand roller aimed at producing this effect. The finer waviness (noise) referred to as roughness is seen in Figure 24b for the recycled pigment based paint film but is absent on the surface profile of the virgin pigment based paint (Figure 24a).

The separation of waviness from roughness was achieved using Vision64 version 5.51 update 2 software. The primary profiles for each paint from Figure 24a-b were filtered so that waves longer than 0.5 mm (called waviness) were removed, while waves shorter than 0.5 mm (called roughness) were displayed. The filtered profiles are shown in Figure 24c for virgin and in Figure 24d recycled pigment based paint. It becomes clear that the roughness of the paint with the recycled pigment is much larger than that of the virgin pigment. However, the surface structure of the application method is more dominant to the overall paint structure than the contribution of the aggregated pigments. This, together with the size of the aggregates, makes the agglomerates hard to detect for an observer beyond 30 cm from the paint film.

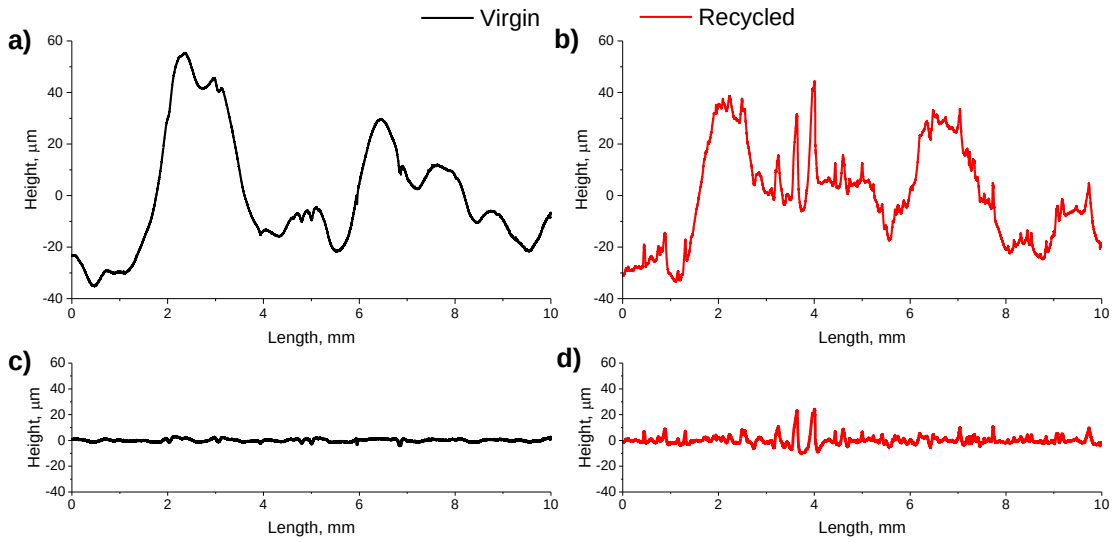

Figure 24 Primary line scan of the stylus profilometer. a) virgin Pigment C and b) recycled Pigment C based paint films. Surface roughness of the line scan for c) virgin Pigment C and d) recycled Pigment C based paint films. Each line scan is 10 mm in length.

5. Summary and conclusions

The overall objective of this work was to extract inorganic pigment, TiO_2, from waste paint for use as the replacement of virgin pigments, in new paint formulations. TiO_2 was recovered from waste paint using a pyrolysis based recycling process from white, water-based decorative paint. Two different heating methods were evaluated for the pyrolysis process: microwave and conventional conduction heating. Waste paint was modelled using a white paint formulation based only on TiO_2 (Paper II, III, IV) or TiO_2 and several different inorganic extender pigments (Paper I). Thermal stability of several common paint components was investigated. The recycled TiO_2 was characterized after the recycling process, and their properties were compared to those of their virgin counterpart. Finally recycled pigments were used as replacement for virgin pigments in paint formulations.

A microwave heated pyrolysis process was evaluated. It was concluded that this works adequately for paints containing a rather high water content. However, for paints where the water content has been reduced, it gave a non-uniform temperature distribution, leaving some of the paint unpyrolysed. Therefore, microwave heated pyrolysis is not suitable for paint waste where a thick dry film has been formed or on fully dried paint. Using conventional heating methods a future recycling process can be designed to be more flexible and handle a wider array of paint waste in different stages of drying.

The thermal stability of commonly used inorganic and organic paint components of decorative paint was investigated using DSC and TGA. From this study it was determined that the optimal pyrolysis temperature for waste paint is approximately 500 °C. At this temperature the degradation of the organic components in the paint occurs while the crystal core of TiO_2 pigments remained intact. Pyrolysis was followed with an oxidation step where the recovered inorganic pigments were oxidized in air to remove residual carbon left after the recycling process improving the colour (whiteness) of the pigment. However, the presence of salts, from degraded paint components, made it necessary to introduce a second purification step were the pigments were purified (washed) with ionic exchanger resins.

XPS results indicated that there were no major changes in the chemical state of the surface species in either pigment (Pigment A, B, and C) analysed in this study after the recycling process. However, the XPS revealed that the thickness of the coating of the pigments was reduced, the best case, or that the chemical composition of the coating, worst case, had been altered. Zeta potential measurements supported the XPS results. The extent to which the coating is degraded depends on the chemistry of the coating. A coating consisting of only Al (Pigment C) or a combination of Al and Zr (Pigment A) is more resistant to degradation in the recycling process than a coating consisting of a combination of Al and Si (Pigment B).

Paint was made using the recycled Pigment C and the properties of the paint were compared to a paint made with virgin pigment. There were no major issues regarding viscosity, pH, or colour with the paint based on recycled Pigment. However, the paint based on recycled pigment had a lower hiding power than the paint based on virgin pigment. One of the main reasons why TiO_2 is used as a pigment is due to its ability to scatter light which makes it possible to produce white paints having a very good hiding power. Even though there was a slight decrease in hiding power for the paint based on recycled pigment compared to the virgin pigment, it was the reduction in gloss and the presence of aggregated pigments in the paint films was the bigger issue. The reduction in gloss turned the formulation from a glossy (virgin pigment) to a mid-sheen formulation (recycled pigment).

The characterization study showed no major differences between virgin and recycled pigments used to produce the paint samples. It is, however, impossible to rule out minor alterations which are hard to quantify, that may have occurred to the surface of the pigment in terms of surface chemistry. These alterations would play a role when it comes to the interaction with the surface active components of a paint leading to, for instance, aggregation, during film forming. This observation also suggests that formulation of paint should be tuned towards the use of recycled pigment, as for any other pigment. Improved milling before or during the incorporation of the recycled pigment into the paint matrix could potentially reduce some of the aggregates.

Even though the recycled pigment gives a quality decrease, its use as a replacement for virgin pigments remains largely possible. In certain applications this drop in performance can be acceptable. When the paint containing the recycled pigment was applied with a roller, it was very hard to identify the agglomerates due to the topography of the rolled paint. Furthermore, the gloss of the formulation based on recycled pigments was higher than most wall and ceiling paints, so an extender pigment would be needed to reduce the gloss even further. This means that the recycled pigment might be of greater value in formulations with lower gloss or sheen, which is one of the currently developing trends in the global decorative paint market. Additionally, the paint based on recycled pigment could be applied to rough surfaces, such as a mineral substrate, without any problems. One other application for the paint could be surfaces that usually do not get scrutinised carefully, such as ceilings.

In the formulation presented in this work, a 100% replacement of virgin pigment with recycled pigment was tested. A smaller replacement would most likely have given less impact on the paint properties. If the recycled pigment is not used as a replacement for TiO_2 pigment in a high gloss paint formulation, it could be used as a so called extender pigment. Extender pigments are used to reduce gloss in, for example, formulations for wall and ceiling paints. Here the recycled pigment would have the benefit of reducing gloss without the trade-off in reduced whiteness or opacity which is normally associated with more traditional extender pigments.

Overall, the results of the present investigation show that it is possible to recycle TiO_2 pigments from paint waste, with minor effects on the paint properties. However, the gloss and covering power of the recycled pigment was lower than that of paint made with the virgin pigment due to pigment aggregation. Agglomeration could probably be mended by further work on formulation, which is expected to be done as for any new pigment product. The performance of the recycled pigment can be deemed as clearly promising by the paint industry which justifies further development in the field. Under ideal circumstances the recycled pigment would be a suitable replacement for virgin pigments in new paint formulations. For the recycling of paint waste and the recovery of TiO_2 pigment by thermal treatment to be a viable option, the resistance of the coating during recycling has to be taken into account at the production stage of the pigment life. It would therefore be beneficial for the pigment producers, the coating industry, and waste handling companies to work in conjunction for further sustainable product development.

6. Future work

The work in this thesis can be seen as proof of concept. It has been proven that TiO_2 can be extracted from a paint matrix, and that the recycled pigment could find a use in certain paint applications. However, there is still a lot of work needed to be done for this process to be successful on a commercial scale.

Further study on the aggregation of pigments after the recycling process is needed. Is it possible that improved milling prior to or during the incorporation of the pigment into the paint matrix could reduce some of the pigment aggregates? One important unanswered question is also if the pigments is already aggregated when it is incorporated into the paint or are aggregates formed when the pigment is introduced into the paint due to pigment incompatibility with some paint component. In this work the interaction between the pigment and other paint components was not studied. Perhaps paint formulations can be altered to enhance the performance of the recycled pigment. There could also potentially be other applications/products more suitable for the recycled pigment than decorative paint.

Another important question not touched upon in this work is how to deal with the other inorganic pigments that undoubtedly will be present in paint waste together with the TiO_2. To separate the TiO_2 from these other pigments could potentially be a rather complicated process, but the first thing that comes to mind is to try some density separation or a flotation process. However, even if the other inorganic pigments are successfully separated away and a pure TiO_2 fraction is produced, it is most likely that it consist of TiO_2 pigments with different surface coatings. It has been shown in this work that differently coated pigments show different tendencies of degradation in the recycling process. Even the most resistant coating showed a slight degradation of the coating that could create the need to recoat the pigment after a couple of recycling cycles. A mix of recycled pigments with different coatings and at different stages of degradation would create an inhomogeneous mix of pigments.

This leads to another important future research topic that must be dealt with. As it is today, at some stage the recycled pigments will need to be recoated with a new surface coating. One of the issues behind the aggregation could be the partial degradation of the surface coating which creates an inhomogeneous surface leading to aggregation. The possibility to develop a more temperature resistant coating could be a future possibility. Or, perhaps the better solution is to produce a coating that is easily broken down in the recycling process to create a more uniform TiO_2 surface that facilitates recoating. It all bottles down to the chemistry of the coating and the coating process needs to be studied further.

There is also a lot of optimization work that needs to be done. Different process parameters such as temperature and residence time of the paint in the pyrolysis process have to be fine-tuned. Could it be possible to include plastic packaging in the pyrolysis process so it does not need to be separated from the paint waste before the recycling process? Alternatives to pyrolysis can be gasification, biological treatment, or to use a solvent to separate the organic fraction from the inorganic fraction of the paint. A life cycle assessment of the process needs to be done to evaluate potential environmental and economic gains of using recycled pigment as replacements for virgin pigments.

7. References

1. Braun, J.H., A. Baidins, and R.E. Marganski, *TiO2 pigment technology: a review*. Progress in Organic Coatings, 1992. **20**(2): p. 105-138.
2. *Chemical Economics Handbook version 2014* [cited 2014 2014-05-05]; Chemical Economics Handbook version 2014]. Available from: http://www.ihs.com/products/chemical/planning/ceh/titanium-dioxide.aspx.
3. Braun, J.H., *Titanium dioxide - A review*. Journal of Coatings Technology, 1997. **69**(868): p. 59-72.
4. Patton, T.C., *Pigment handbook. Vol. 3, Characterization and physical relationships*. 1973, New York: Wiley.
5. Solomon, D.H. and D.G. Hawthorne, *Chemistry of pigments and fillers*. 1983, New York ;: Wiley.
6. Parfitt, G.D., *The role of the surface in the behavior of titanium dioxide pigments.* Croat. Chem. Acta, 1980. **53**(2): p. 333-9.
7. Middlemas, S., Z.Z. Fang, and P. Fan, *LCA comparison of emerging and traditional TiO2 manufacturing processes.* J. Cleaner Prod., 2015. **89**: p. 137-147.
8. *COMMISSION DECISION of 28 May 2014 establishing the ecological criteria for the award of the EU Ecolabel for indoor and outdoor paints and varnishes*, T.E. COMMISSION, Editor. 2014.
9. Jiannis S. Kougoulis, R.K., Ben Walsh, Katherine Bojczuk, Trevor Crichton *Revision of EU European Ecolabel and Development of EU Green Public Procurement Criteria for Indoor and Outdoor Paints and Varnishes*. 2012.
10. Ruszala, M.J.A., N.A. Rowson, L.M. Grover, and R.A. Choudhery, *Low carbon footprint TiO2 substitutes in paint: a review.* Int. J. Chem. Eng. Appl., 2015. **6**(5): p. 331-340.
11. TZMI, *Introduction to the titanium and zirconium value chains*. 2013.
12. U.S. Geological Survey, *Mineral commodity summaries 2017*. 2017. p. 177-179.
13. Patton, T.C. and P.A. Lewis, *Pigment handbook. Vol. 1, Properties and economics*. 1988, New York: Wiley.
14. Buxbaum, G., *Industrial inorganic pigments*. 3nd completely rev. ed. 2005, Weinheim ; New York: Wiley-VCH. xv, 300 s. : ill.
15. Agrios, A.G. and P. Pichat, *State of the art and perspectives on materials and applications of photocatalysis over TiO2.* Journal of Applied Electrochemistry, 2005. **35**(7): p. 655-663.
16. Talbert, R., *Paint Technology Handbook [Elektronisk resurs]*. 2007, Hoboken: Taylor & Francis Ltd.
17. Lambourne, R. and T.A. Strivens, *Paint and Surface Coatings - Theory and Practice (2nd Edition)*. 1999, Woodhead Publishing.
18. Turner, G.P.A. and J. Bentley, *Introduction to paint chemistry: and principles of paint technology*. 4. ed ed. 1998.
19. Weldon, D.G., *Failure Analysis of Paints and Coatings (Revised Edition)*. John Wiley & Sons.
20. *Industrial Minerals and Their Uses - A Handbook and Formulary [Elektronisk resurs]*. 1996: William Andrew Publishing/Noyes.
21. Morris, G.E., W.A. Skinner, P.G. Self, and R.S.C. Smart, *Surface chemistry and rheological behaviour of titania pigment suspensions.* Colloids and Surfaces A: Physicochemical and Engineering Aspects, 1999. **155**(1): p. 27-41.
22. Swiler, D.R., *Pigments, Inorganic*, in *Kirk-Othmer Encyclopedia of Chemical Technology*. 2000, John Wiley & Sons, Inc.
23. Parfitt, G.D. and K.S.W. Sing, *Characterization of powder surfaces : with special reference to pigments and fillers*. 1976, London: Academic P.
24. Wicks, Z.W., *Coatings*, in *Kirk-Othmer Encyclopedia of Chemical Technology*. 2000, John Wiley & Sons, Inc.
25. Parfitt, G.D., *Dispersion of powders in liquids : with special reference to pigments*. 1981, London: Applied Science Publishers.

26. Tadros, T.F., *Colloids in Paints: Colloids and Interface Science, Volume 6*. 2010, Weinheim: John Wiley & Sons.
27. Abrahao, R.T., V. Postal, J.L. Paiva, and R. Guardani, *Wettability study for pigmentary titanium dioxide.* J. Coat. Technol. Res., 2013. **10**(6): p. 829-840.
28. Kronberg, B., K. Holmberg, and B. Lindman, *Surface chemistry of surfactants and polymers*. 2014, Chichester: Wiley.
29. Derjaguin, B. and L. Landau, *Theory of the stability of strongly charged lyophobic sols and of the adhesion of strongly charged particles in solutions of electrolytes.* Progress in Surface Science, 1993. **43**(1): p. 30-59.
30. Verwey, E.J.W. and J.T.G. Overbeek, *Theory of the Stability of Lyophobic Colloids*. 1948: Elsvier Pub. Co. 216 pp.
31. Croll, S., *DLVO theory applied to TiO2 pigments and other materials in latex paints.* Progress in Organic Coatings, 2002. **44**(2): p. 131-146.
32. Berg, J.C., *An introduction to interfaces & colloids : the bridge to nanoscience*. 2010, Singapore: World Scientific.
33. Bieleman, J., *Additives for coatings*. 2000, Weinheim: Wiley-VCH.
34. Sun, C. and J.C. Berg, *A review of the different techniques for solid surface acid–base characterization.* Advances in Colloid and Interface Science, 2003. **105**(1–3): p. 151-175.
35. Schacht, C.A., *Refractories handbook*. Mechanical engineering (Marcel Dekker, Inc.), 99-0151599-8 ; 178. 2004, New York: Marcel Dekker.
36. Stokes, R.J. and D.F. Evans, *Fundamentals of interfacial engineering*. Advances in interfacial engineering series, 99-1578130-X. 1997, New York: Wiley-VCH.
37. Buscall, R., *The Hamaker coefficient for titanium dioxide (rutile) in liquid media.* Colloids and Surfaces A: Physicochemical and Engineering Aspects, 1993. **75**: p. 269-272.
38. Ackler, H.D., R.H. French, and Y.-M. Chiang, *Comparisons of Hamaker Constants for Ceramic Systems with Intervening Vacuum or Water: From Force Laws and Physical Properties.* Journal of Colloid and Interface Science, 1996. **179**(2): p. 460-469.
39. Kosmulski, M., *Chemical properties of material surfaces*. Surfactants science series, 0081-9603 ; 102. 2001, New York: Dekker.
40. Franks, G.V. and Y. Gan, *Charging Behavior at the Alumina–Water Interface and Implications for Ceramic Processing.* Journal of the American Ceramic Society, 2007. **90**(11): p. 3373-3388.
41. O'Brien, R.W., *Electro-acoustic effects in a dilute suspension of spherical particles.* Journal of Fluid Mechanics, 1988. **190**: p. 71-86.
42. O'Brien, R.W., *The electroacoustic equations for a colloidal suspension.* Journal of Fluid Mechanics, 1990. **212**: p. 81-93.
43. Předota, M., M.L. Machesky, and D.J. Wesolowski, *Molecular Origins of the Zeta Potential.* Langmuir, 2016. **32**(40): p. 10189-10198.
44. Lyklema, J., *Surface charges and electrokinetic charges: Distinctions and juxtapositionings.* Colloids and Surfaces A: Physicochemical and Engineering Aspects, 2011. **376**(1–3): p. 2-8.
45. Kosmulski, M., *Surface charging and points of zero charge*. Surfactant science series, 0081-9603 ; 145. 2009, Boca Raton: CRC Press.
46. Diebold, M.P., *Application of Light Scattering to Coatings: A User's Guide*. 2014: Springer International Publishing.
47. Wiese, G.R. and T.W. Healy, *Coagulation and electrokinetic behavior of TiO2 and Al2O3 colloidal dispersions.* Journal of Colloid and Interface Science, 1975. **51**(3): p. 427-433.
48. van der Donck, J.C.J., G.E.J. Vaessen, and H.N. Stein, *Adsorption of short-chain tetraalkylammonium bromide on silica.* Langmuir, 1993. **9**(12): p. 3553-3557.
49. SAKAB. *Om farligt avfall*. [cited 2014 2014-06-03]; Available from: http://www.sakab.se/sites/default/files/attachment/vitbok_om-farligt_avfall.pdf.
50. Fjelsted, L. and T.H. Christensen, *Household hazardous waste: composition of paint waste.* Waste Management & Research, 2007. **25**(6): p. 502-509.
51. Stockholmsregionens avfallsråd. [cited 2018 2018-02-19]; Available from: http://www.atervinningscentralen.se/web/page.aspx?refid=93.
52. RebornPaints. [cited 2014 2014-05-05]; Available from: http://www.rebornpaints.co.uk/.

53. CommunitePaints. [cited 2014 2014-05-05]; Available from: http://www.communityrepaint.org.uk/.
54. Muniz, L.A.R., A.R. Costa, E. Steffani, A.J. Zattera, K. Hofsetz, K. Bossardi, and L. Valentini, *A study of paint sludge deactivation by pyrolysis reactions.* Brazilian Journal of Chemical Engineering, 2003. **20**: p. 63-68.
55. Januri, Z., N.A. Rahman, S.S. Idris, S. Matali, and S.F.A. Manaf, *Yields performance of automotive paint sludge via microwave assisted pyrolysis*, in *Applied Mechanics and Materials*. 2014. p. 191-195.
56. Kim, B.R., E.M. Kalis, I.T. Salmeen, C.W. Kruse, I. Demir, S.L. Carlson, and M. Rostam-Abadi, *Evaluating paint-sludge chars for adsorption of selected paint solvents.* Journal of Environmental Engineering, 1996. **122**(6): p. 532-539.
57. Nakouzi, S., D. Mielewski, J.C. Ball, B.R. Kim, I.T. Salmeen, D. Bauer, and C.K. Narula, *A novel approach to paint sludge recycling: Reclaiming of paint sludge components as ceramic composites and their applications in reinforcement of metals and polymers.* Journal of Materials Research, 1998. **13**(1): p. 53-60.
58. Gerace, M.J., S.C. Gamboa, and Y.S. Landaburu, *Method of making sludge powder and sealant from paint sludge and sludge powder and sealant compositions produced thereby*. 1993, Google Patents.
59. Dixon, D.M., D.A. Fischer, R.R. Matheson, and J.R. Moore, *Process for producing building materials from raw paint sludge*. 2005, Google Patents.
60. Sanghvi, H. and J.L. Massingill, *Recycling paint overspray*. Journal of Coatings Technology, 2002. **74**(933): p. 143-145.
61. Seyed Mostafa, K., S. Seyed Mahmood, and T. Sahar, *Evaluation of extracting titanium dioxide from water-based paint sludge in auto-manufacturing industries and its application in paint production.* Toxicology and Industrial Health, 2012. **29**(8): p. 697-703.
62. Rezaiyan, J. and N.P. Cheremisinoff, *Gasification technologies : a primer for engineers and scientists*. 2005, Boca Raton, FL : CRC Press.
63. Williams, P.T., *Waste treatment and disposal*. 1998, Chichester: Wiley.
64. Andrea Undri, L.R., Marco Frediani and Piero Frediani, *Microwave pyrolysis of polymeric materials*, in *Microwave Heating*, D.U. Chandra, Editor. 2011.
65. Menéndez, J.A., M. Inguanzo, and J.J. Pis, *Microwave-induced pyrolysis of sewage sludge.* Water Research, 2002. **36**(13): p. 3261-3264.
66. Ludlow-Palafox, C. and H.A. Chase, *Microwave-Induced Pyrolysis of Plastic Wastes.* Industrial & Engineering Chemistry Research, 2001. **40**(22): p. 4749-4756.
67. Appleton, T.J., R.I. Colder, S.W. Kingman, I.S. Lowndes, and A.G. Read, *Microwave technology for energy-efficient processing of waste.* Applied Energy, 2005. **81**(1): p. 85-113.
68. Clark, D.E., D.C. Folz, and J.K. West, *Processing materials with microwave energy.* Materials Science and Engineering: A, 2000. **287**(2): p. 153-158.
69. Haque, K.E., *Microwave energy for mineral treatment processes—a brief review.* International Journal of Mineral Processing, 1999. **57**(1): p. 1-24.
70. Jones, D.A., T.P. Lelyveld, S.D. Mavrofidis, S.W. Kingman, and N.J. Miles, *Microwave heating applications in environmental engineering - A review.* Resources, Conservation and Recycling, 2002. **34**(2): p. 75-90.
71. JCPDS-ICCD:PDF-4, *Joint Committee of Powder Diffraction Standards*. 2013.
72. Andersson, M., M. Knutson Wedel, C. Forsgren, and J. Christéen, *Microwave assisted pyrolysis of residual fractions of waste electrical and electronics equipment.* Minerals Engineering, 2012. **29**(0): p. 105-111.
73. Brunauer, S., P.H. Emmett, and E. Teller, *Adsorption of Gases in Multimolecular Layers.* Journal of the American Chemical Society, 1938. **60**(2): p. 309-319.
74. Urwin, D., *Surface area and porosity of titanium dioxide pigments.* J. Oil Colour Chem. Ass., 1969. **52**(8): p. 697-710.
75. Farrokhpay, S., *A review of polymeric dispersant stabilisation of titania pigment.* Advances in Colloid and Interface Science, 2009. **151**(1–2): p. 24-32.
76. Egerton, T.A., G.D. Parfitt, Y. Kang, and J.P. Wightman, *XPS analysis of uncoated and silica-coated titanium dioxide powders.* Colloids and Surfaces, 1983. **7**(4): p. 311-323.

77. Jillavenkatesa, A., S.J. Dapkunas, and L.-S.H. Lum, *Particle Size Characterization*. NIST Recommended Practice Guide. 2001: National Institute of Standards and Technology.
78. O'Brien, R.W., D.W. Cannon, and W.N. Rowlands, *Electroacoustic Determination of Particle Size and Zeta Potential.* Journal of Colloid and Interface Science, 1995. **173**(2): p. 406-418.
79. Patton, T.C., *Paint flow and pigment dispersion*. 1964, New York: Interscience.
80. Koleske, J.V., *Paint and Coating Testing Manual - Fifteenth Edition of the Gardner-Sward Handbook: (MNL 17-2nd)*. ASTM International.
81. *Colorimetry –Part 4: CIE 1976 L*a*b* Colour space (ISO 11664-4:2008).*
82. *Colorimetry –Part 6: CIEDE2000 Colour-difference formula (ISO / CIE 11664-6:2014).*
83. Sababi, M., J. Kettle, H. Rautkoski, P.M. Claesson, and E. Thormann, *Structural and Nanomechanical Properties of Paperboard Coatings Studied by Peak Force Tapping Atomic Force Microscopy.* ACS Applied Materials & Interfaces, 2012. **4**(10): p. 5534-5541.
84. Foster, B., *New Atomic Force Microscopy (AFM) Approaches Life Science Gently, Quantitatively, and Correlatively.* American Laboratory, 2012. **44**: p. 4.
85. Samtani, M., D. Dollimore, and K.S. Alexander, *Comparison of dolomite decomposition kinetics with related carbonates and the effect of procedural variables on its kinetic parameters.* Thermochimica Acta, 2002. **392-393**: p. 135-145.
86. Gunasekaran, S. and G. Anbalagan, *Thermal decomposition of natural dolomite.* Bulletin of Materials Science, 2007. **30**(4): p. 339-344.
87. Clark, R.J.H., D.C. Bradley, and P. Thornton, *The Chemistry of Titanium*. Pergamon texts in inorganic chemistry, 99-0125710-7 ; 19. 1973, Oxford: Pergamon press.
88. Burfield, D.R., *Compositional analysis of waterborne paint systems by thermogravimetry.* Thermochimica Acta, 1986. **106**(C): p. 79-91.
89. Day, R.E., *The characterisation of the surface of titanium dioxide pigments.* Progress in Organic Coatings, 1974. **2**(4): p. 269-288.
90. Brindley, G.W. and M. Nakahira, *The Kaolinite-Mullite Reaction Series: II, Metakaolin.* Journal of the American Ceramic Society, 1959. **42**(7): p. 314-318.
91. Brindley, G.W. and M. Nakahira, *The KaoIinite-MuIIite Reaction Series: Ill, The High-Temperature Phases.* Journal of the American Ceramic Society, 1959. **42**(7): p. 319-324.
92. Ptáček, P., D. Kubátová, J. Havlica, J. Brandštetr, F. Šoukal, and T. Opravil, *Isothermal kinetic analysis of the thermal decomposition of kaolinite: The thermogravimetric study.* Thermochimica Acta, 2010. **501**(1–2): p. 24-29.
93. Guggenheim, S., Y.H. Chang, and A.F. Koster Van Groos, *Muscovite dehydroxylation: high-temperature studies.* American Mineralogist, 1987. **72**(5-6): p. 537-550.
94. Mazzucato, E., G. Artioli, and A. Gualtieri, *High temperature dehydroxylation of muscovite-2M1: A kinetic study by in situ XRPD.* Physics and Chemistry of Minerals, 1999. **26**(5): p. 375-381.
95. Wesołowski, M., *Thermal decomposition of talc: A review.* Thermochimica Acta, 1984. **78**(1-3): p. 395-421.
96. *ISO 6504-3:2006 Paints and varnishes -- Determination of hiding power -- Part 3: Determination of contrast ratio of light-coloured paints at a fixed spreading rate*. 2009-04-02.
97. *ASTM E313 Standard Practice for Calculating Yellowness and Whiteness Indices from Instrumentally Measured Color Coordinates*.
98. *ISO 2813:1994 Paints and varnishes -- Determination of specular gloss of non-metallic paint films at 20 degrees, 60 degrees and 85 degrees*.
99. *ISO 11998:2006 Paints and varnishes -- Determination of wet-scrub resistance and cleanability of coatings*.
100. Kumar, P.M., S. Badrinarayanan, and M. Sastry, *Nanocrystalline TiO2 studied by optical, FTIR and X-ray photoelectron spectroscopy: correlation to presence of surface states.* Thin Solid Films, 2000. **358**(1): p. 122-130.
101. Sherwood, P.M.A., *Introduction to Studies of Aluminum and its Compounds by XPS.* Surface Science Spectra, 1998. **5**(1): p. 1-3.
102. Kloprogge, J.T., L.V. Duong, B.J. Wood, and R.L. Frost, *XPS study of the major minerals in bauxite: Gibbsite, bayerite and (pseudo-)boehmite.* Journal of Colloid and Interface Science, 2006. **296**(2): p. 572-576.

103. Alexander, M.R., G.E. Thompson, and G. Beamson, *Characterization of the oxide/hydroxide surface of aluminium using x-ray photoelectron spectroscopy: a procedure for curve fitting the O 1s core level.* Surf. Interface Anal., 2000. **29**(7): p. 468-477.
104. Lo, P.-H., W.-T. Tsai, J.-T. Lee, and M.-P. Hung, *The electrochemical behavior of electroless plated Ni-P alloys in concentrated NaOH solution.* J. Electrochem. Soc., 1995. **142**(1): p. 91-6.
105. Banach, M. and A. Makara, *Thermal Decomposition of Sodium Phosphates.* Journal of Chemical & Engineering Data, 2011. **56**(7): p. 3095-3099.
106. Morant, C., J.M. Sanz, L. Galán, L. Soriano, and F. Rueda, *An XPS study of the interaction of oxygen with zirconium.* Surface Science, 1989. **218**(2): p. 331-345.
107. Barreca, D., G.A. Battiston, R. Gerbasi, E. Tondello, and P. Zanella, *Zirconium Dioxide Thin Films Characterized by XPS.* Surface Science Spectra, 2000. **7**(4): p. 303-309.
108. Losoi, T., *Surface studies of titanium dioxide pigments.* J. Coat. Technol., 1989. **61**(776): p. 57-63.
109. Siwinska-Stefanska, K., A. Krysztafkiewicz, and T. Jesionowski, *Effect of inorganic oxides treatment on the titanium dioxide surface properties.* Physicochem. Probl. Miner. Process., 2008. **42**: p. 141-151.
110. Taylor, M.L., G.E. Morris, and R.S.C. Smart, *Influence of aluminum doping on titania pigment structural and dispersion properties.* Journal of Colloid and Interface Science, 2003. **262**(1): p. 81-88.
111. Queeney, K.T., M.K. Weldon, J.P. Chang, Y.J. Chabal, A.B. Gurevich, J. Sapjeta, and R.L. Opila, *Infrared spectroscopic analysis of the Si/SiO2 interface structure of thermally oxidized silicon.* Journal of Applied Physics, 2000. **87**(3): p. 1322-1330.
112. Barr, T.L., S. Seal, H. He, and J. Klinowski, *X-ray photoelectron spectroscopic studies of kaolinite and montmorillonite.* Vacuum, 1995. **46**(12): p. 1391-1395.
113. Wang, L., Z. Wang, H. Yang, and G. Yang, *The study of thermal stability of the SiO2 powders with high specific surface area.* Materials Chemistry and Physics, 1999. **57**(3): p. 260-263.
114. Dementjev, A.P., O.P. Ivanova, L.A. Vasilyev, A.V. Naumkin, D.M. Nemirovsky, and D.Y. Shalaev, *Altered layer as sensitive initial chemical state indicator.* J. Vac. Sci. Technol., A, 1994. **12**(2): p. 423-7.
115. Alexander, M.R., R.D. Short, F.R. Jones, M. Stollenwerk, J. Zabold, and W. Michaeli, *An x-ray photoelectron spectroscopic investigation into the chemical structure of deposits formed from hexamethyldisiloxane/oxygen plasmas.* J. Mater. Sci., 1996. **31**(7): p. 1879-85.
116. Camino, G., S.M. Lomakin, and M. Lazzari, *Polydimethylsiloxane thermal degradation Part 1. Kinetic aspects.* Polymer, 2000. **42**(6): p. 2395-2402.
117. Perron, H., J. Vandenborre, C. Domain, R. Drot, J. Roques, E. Simoni, J.J. Ehrhardt, and H. Catalette, *Combined investigation of water sorption on TiO2 rutile (110) single crystal face: XPS vs. periodic DFT.* Surface Science, 2007. **601**(2): p. 518-527.
118. McCafferty, E. and J.P. Wightman, *Determination of the concentration of surface hydroxyl groups on metal oxide films by a quantitative XPS method.* Surface and Interface Analysis, 1998. **26**(8): p. 549-564.
119. Boisvert, J.-P., J. Persello, J.-C. Castaing, and B. Cabane, *Dispersion of alumina-coated TiO2 particles by adsorption of sodium polyacrylate.* Colloids and Surfaces A: Physicochemical and Engineering Aspects, 2001. **178**(1–3): p. 187-198.
120. Farrokhpay, S., G.E. Morris, D. Fornasiero, and P. Self, *Influence of polymer functional group architecture on titania pigment dispersion.* Colloids and Surfaces A: Physicochemical and Engineering Aspects, 2005. **253**(1–3): p. 183-191.
121. Zhuravlev, L.T., *The surface chemistry of amorphous silica. Zhuravlev model.* Colloids and Surfaces A: Physicochemical and Engineering Aspects, 2000. **173**(1): p. 1-38.
122. Parks, G.A., *The Isoelectric Points of Solid Oxides, Solid Hydroxides, and Aqueous Hydroxo Complex Systems.* Chemical Reviews, 1965. **65**(2): p. 177-198.
123. Primet, M., P. Pichat, and M.V. Mathieu, *Infrared study of the surface of titanium dioxides. I. Hydroxyl groups.* The Journal of Physical Chemistry, 1971. **75**(9): p. 1216-1220.

124. Nsib, F., N. Ayed, and Y. Chevalier, *Comparative study of the dispersion of three oxide pigments with sodium polymethacrylate dispersants in alkaline medium.* Progress in Organic Coatings, 2007. **60**(4): p. 267-280.
125. Srinivasa Rao, A., *Effect of pH on the suspension stability of alumina, titania and their mixtures.* Ceramics International, 1987. **13**(4): p. 233-241.
126. Lefèvre, G., M. Duc, P. Lepeut, R. Caplain, and M. Fédoroff, *Hydration of γ-Alumina in Water and Its Effects on Surface Reactivity.* Langmuir, 2002. **18**(20): p. 7530-7537.